

✓  
Conf-

790301-16

METAL HYDRIDE TECHNOLOGY\*

J. J. Reilly  
Department of Energy and Environment  
Brookhaven National Laboratory  
Upton, New York 11973

**MASTER**

February 1979

NOTICE

This report was prepared as an account of work sponsored by the United States Government. Neither the United States nor the United States Department of Energy, nor any of their employees, nor any of their contractors, subcontractors, or their employees, makes any warranty, express or implied, or assumes any legal liability or responsibility for the accuracy, completeness or usefulness of any information, apparatus, product or process disclosed, or represents that its use would not infringe privately owned rights.

\*This work was supported by the Division of Chemical Sciences, U.S. Department of Energy, Washington, D.C., under Contract #EY76-C-02-0016.

## **DISCLAIMER**

**This report was prepared as an account of work sponsored by an agency of the United States Government. Neither the United States Government nor any agency Thereof, nor any of their employees, makes any warranty, express or implied, or assumes any legal liability or responsibility for the accuracy, completeness, or usefulness of any information, apparatus, product, or process disclosed, or represents that its use would not infringe privately owned rights. Reference herein to any specific commercial product, process, or service by trade name, trademark, manufacturer, or otherwise does not necessarily constitute or imply its endorsement, recommendation, or favoring by the United States Government or any agency thereof. The views and opinions of authors expressed herein do not necessarily state or reflect those of the United States Government or any agency thereof.**

## **DISCLAIMER**

**Portions of this document may be illegible in electronic image products. Images are produced from the best available original document.**

## METAL HYDRIDE TECHNOLOGY

J. J. Reilly  
Department of Energy and Environment  
Brookhaven National Laboratory  
Upton, New York 11973

Hydrogen has certain properties which make it a most attractive fuel. It can be used in a variety of energy converters, it is non-polluting and can be made from readily available raw materials and/or energy sources. Unfortunately, the difficulties involved in its convenient storage have prevented its widespread use as a common, ordinary fuel. Currently, hydrogen is stored either as a compressed gas or as a cryogenic liquid; however, neither method is a feasible option in this context. A promising alternative is storage as a metal hydride. Indeed, it is this promise which has been responsible for the recent upsurge of interest in metal-hydrogen systems and it is the purpose of this review to summarize the properties and applications of those systems which have proven or potential utility as hydrogen storage compounds.

### A. PROPERTIES

#### I.A General

Metal hydride compounds may be divided into three general categories: ionic, metallic and covalent.<sup>1</sup> The classification is based on the predominant character of the hydrogen bond and is somewhat equivocal since no one compound exhibits purely one type of bonding. Unlike the ionic and metallic hydrides, the covalent hydrides can be eliminated from consideration because they cannot be formed by the direct reaction of hydrogen with the metal except under very special conditions. The ionic hydrides, with the possible exception of magnesium hydride, are too stable for use in practical hydrogen storage systems and it is the primarily metallic hydrides which are of interest. Unfortunately, de-

spite the fact that most elemental metals will react directly and reversibly with hydrogen, only magnesium hydride ( $\text{MgH}_2$ ) and possibly vanadium hydride ( $\text{VH}_2$ ) could be useful from an energy storage point of view; all of the others can be eliminated for reasons of cost and/or stability. However, it has been shown that many alloys or intermetallic compounds will react directly and reversibly with hydrogen to form distinct hydride phases which, in many cases, have properties that are quite different than those of the binary hydrides of the individual alloy components. Indeed, most of the recent work concerned with hydrogen storage compounds has been focused on ternary hydrides formed by such reactions. Thus, it is appropriate to state three general rules which these systems obey:<sup>21</sup>

1. In order for an intermetallic compound to react directly and reversibly with hydrogen to form a distinct hydride phase, it is necessary that at least one of the metal components be capable of reacting directly and reversibly with hydrogen to form a stable binary hydride.

2. If a reaction takes place at a temperature at which the metal atoms are mobile, the system will assume its most favored thermodynamic configuration.

3. If the metal atoms are not mobile (as is the case in low temperature reactions), only hydride phases can result which are structurally very similar to the starting intermetallic compound.

Rule 1 is purely empirical and is based on experimental observation.<sup>2,3</sup> The latter two rules are firmly based on established thermodynamic and structural principles. They are, obviously, not new concepts. They refer to two temperature dependent variables, the free energy and the metal atom diffusion rate, either of which may be the dominant factor in system behavior. We believe the

explicit statement of these rules to be quite useful. Their application will be illustrated where appropriate in this review.

At this point we wish to briefly discuss two empirical hypotheses which have been quite helpful in predicting the behavior of alloy hydrides. The first hypothesis is based on a model originally devised by Miedema to predict the heat of formation of alloys and intermetallic compounds<sup>4</sup> and is commonly referred to as the rule of reversed stability.<sup>5</sup> For a detailed exposition, the reader is referred to the literature cited; here we shall merely note that the model states that the enthalpy ( $\Delta H$ ) of formation of a ternary hydride from an intermetallic compound (not from the elements) is composed of three terms:

$$\Delta H_{AB_n H_{2m}} = \Delta H_{AH_m} + \Delta H_{B_n H_m} - \Delta H_{AB_n} \quad (1)$$

where A and B are metals and A is a stable hydride former.

The theory has been quite successful when applied to systems involving the rare earth-transition metal intermetallic compounds, but has been less successful with systems involving Ti alloy hydrides.<sup>6,29</sup>

The second hypothesis, which has been quite helpful in predicting the trend in  $\Delta G_f$  (plateau region) for a homologous series of alloy hydrides, consists of a correlation of  $\Delta G_f$  with the volume of the interstitial site which the hydrogen atom occupies. This correlation is based on the thesis that as the volume of the interstitial site increases, the more readily it will accommodate the hydrogen atom,<sup>7</sup> i.e.,  $\Delta G_f$  will become more negative. A number of investigators have experimentally noted this effect and it has been recently extended and exploited to prepare complex alloy hydrides having predictable and desirable temperature-pressure characteristics for specific applications.<sup>8,9</sup>

There is one further general consideration which should be addressed. In the present context, the most important technical characteristic of any metal-hydrogen system is the interrelationship of its associated pressure-temperature-composition properties. These properties are conveniently summarized in a P-T-C diagram of which an idealized version is shown in Figure 1. It consists of a family of isotherms which shows the variation of the equilibrium pressure with the concentration of hydrogen in the solid. Initially the isotherm ascends steeply as hydrogen dissolves in the metal. This single solid phase region is usually designated as the  $\alpha$  phase of the hydrogen-metal system. Ideally, the isotherm in any single solid-phase region will obey Sievert's law, which states that the concentration of hydrogen in the solid phase is proportional to the square root of the equilibrium pressure, P, i.e.,

$$H_{\text{solid}} = KP^{1/2} \quad (2)$$

Point A in the isotherm marks the terminal solubility of hydrogen in the  $\alpha$  phase and also the appearance of a distinct metal hydride or  $\beta$  phase. It may be recalled that the solubility of hydrogen in many metals can be appreciable; thus, many metal hydrides are quite nonstoichiometric. This is particularly true of those with metallic bonding. Upon the appearance of a second solid phase, the hydrogen pressure remains constant and forms a "plateau" as more hydrogen is added. The pressure plateau persists as long as two distinct solid phases coexist and is a consequence of Gibbs phase rule.

The effect of increasing temperature is shown by the higher temperature isotherms  $T_2$  and  $T_3$ . As the temperature rises, the miscibility gap tends to narrow, accompanied by a consequent reduction in the plateau length. Eventually, at some critical (consolute) temperature, the miscibility gap and the pressure plateau may disappear and the  $\alpha$  phase will convert continuously into a hydride

phase. More than one hydride phase may occur in certain systems, in which case a second and higher plateau may appear. If so, the same considerations apply. In practical terms, the appearance of the pressure plateau is essential since it is the length of this plateau which represents the effective hydrogen storage capacity of the system. In many cases, the plateau has a slight upward slope as the hydrogen content increases; this is usually not of any consequence. However, most systems also depart from ideality by exhibiting a hysteresis effect in the plateau region which, if excessive, can rule out a system in certain applications, e.g. heat pump cycles.

## B. SPECIFIC SYSTEMS

### II.B Magnesium Alloy Hydrides

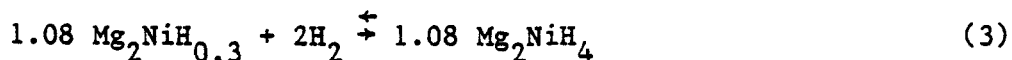
Magnesium hydride ( $\text{MgH}_2$ )<sup>10</sup> contains by weight 7.7% hydrogen. Unfortunately, it is relatively stable having a dissociation pressure of 1 atm at 286°C which is barely within the useful range.<sup>11</sup> Thus, early work turned toward the reaction of hydrogen with magnesium intermetallic compounds; two of these are of interest:  $\text{Mg}_2\text{Ni}$  and  $\text{Mg}_2\text{Cu}$ .

The phase diagram of the Mg-Ni system indicates the existence of two intermetallic compounds,  $\text{Mg}_2\text{Ni}$  and  $\text{MgNi}_2$ .<sup>12</sup> The latter does not react with hydrogen at pressures up to 540 atm in the temperature range -196° to 300°C. However,  $\text{Mg}_2\text{Ni}$  will react with hydrogen to form the ternary hydride,  $\text{Mg}_2\text{NiH}_4$ ,<sup>11</sup> even at room temperature; at 200° and a pressure of 14 atm, it will react rapidly.

A series of pressure-composition isotherms for this system is shown in Figure 2. The abrupt termination of the isotherms at a composition corresponding to  $\text{Mg}_2\text{NiH}_4$  indicates that the hydride has a well defined stoichiometry. The maximum solubility of hydrogen in the  $\alpha$  phase corresponds to a composition of



MgNiH<sub>0.3</sub>. The reaction, starting with the hydrogen saturated alloy may be written as:



The product is a fine powder and has a rust-colored, non-metallic appearance. It is stable in air at room temperature for long periods, but may slowly darken over a period of years (in a glass container). It reacts only slowly when immersed in water, but vigorously with dilute mineral acids. Other pertinent properties of this hydride are listed in Table 1.

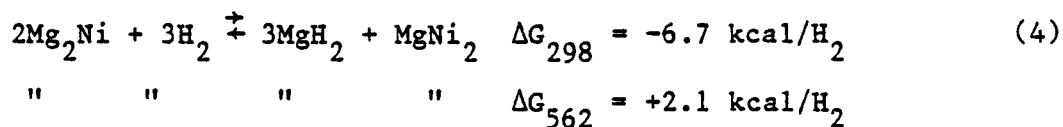
Unlike pure magnesium, both the synthesis and decomposition of Mg<sub>2</sub>NiH<sub>4</sub> are relatively rapid at a temperature above 200°C. The decomposition reaction has been reported to be first order with the rate constants noted below.<sup>13</sup>

Table 2. Decomposition of Mg<sub>2</sub>NiH<sub>4</sub>

| <u>Temp. °C</u> | <u>First Order</u>                        |  |
|-----------------|---|--|
|                 | <u>Rate Constant K</u>                    |  |
| 201             | 7 x 10 <sup>-4</sup> sec <sup>-1</sup>    |  |
| 227             | 7.0 x 10 <sup>-3</sup> sec <sup>-1</sup>  |  |
| 240             | 1.48 x 10 <sup>-2</sup> sec <sup>-1</sup> |  |

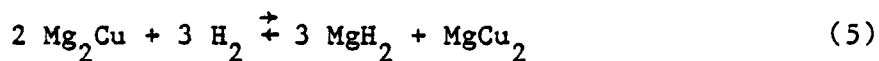
In itself, Mg<sub>2</sub>NiH<sub>4</sub> is not very attractive as an energy storage compound. It contains less than one-half the amount, by weight, of hydrogen in MgH<sub>2</sub> with only a small decrease in stability; its primary virtue lies in the fact that Mg<sub>2</sub>Ni acts as a catalyst for the Mg-H reaction.<sup>11</sup>

It is rather interesting to note that the disproportionation of Mg<sub>2</sub>Ni, as shown below, is as equally favored as reaction (3) at room temperature but becomes less so as the temperature is increased.



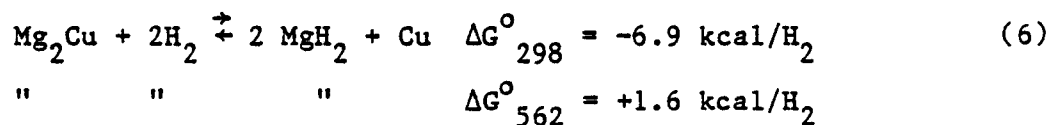
This is a consequence of the slightly more negative entropy of formation of MgH<sub>2</sub> and its relatively low stability as compared to most binary hydrides. If MgH<sub>2</sub> were more stable (by at least several kcal), then reaction (4) would be favored at room temperature and at elevated temperatures the disproportionation of Mg<sub>2</sub>Ni would be a distinct possibility. Indeed this is exactly the situation with many unstable ternary hydrides in which one component forms a stable binary hydride such as titanium. This will be illustrated in Section IIB with several Ti alloy-hydrogen systems.

Despite a structural similarity with Mg<sub>2</sub>Ni, Mg<sub>2</sub>Cu behaves quite differently;<sup>14</sup> it disproportionates to form the binary hydride and a lower intermetallic compound.

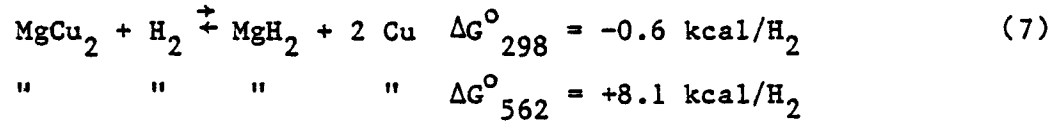


Pertinent thermodynamic quantities for this reaction are  $\Delta H_{298} = -17.4$  kcal,  $\Delta G_{298} = -7.3$  kcal/mol H<sub>2</sub> and  $\Delta S = -34$  e.u./mol H<sub>2</sub>. While this system is somewhat more unstable than the corresponding Mg-H system, it contains only ~2.7 weight % hydrogen vs. 7.6 weight % for the latter. As with the previous system, it is a rather large penalty to pay for only a marginal decrease in stability.

It is worthwhile to analyze the behavior of Mg<sub>2</sub>Cu and hydrogen using rules 2 and 3 noted above. Reaction (5) occurs at reasonable rates at temperatures above 200°C; it is quite rapid at 250°C. No reaction occurs at room temperature at pressures up to 880 atm, as predicted by rule 3. Nor does a ternary hydride form, which would be permitted as it would not require substantial rearrangement of the metal atoms. Another point involves the following hypothetical reaction:



This reaction would be of practical interest since all of the Mg is used to form  $MgH_2$  resulting in a substantial increase in hydrogen storage capacity. Further, since  $\Delta G$  is more positive, the equilibrium pressure would be higher. Both effects are in the desired direction. However, reaction (6) can be considered the sum of reaction (5) and the following:



This reaction will not occur at room temperature (rule 3) and at  $562^{\circ}K$ , where the mobility of the metal atoms has greatly increased,  $\Delta G^{\circ}$  is unfavorable by an amount which corresponds to an equilibrium pressure of 1450 atm. Obviously for energy storage purposes we shall have to be satisfied with the system as represented by reaction (5).

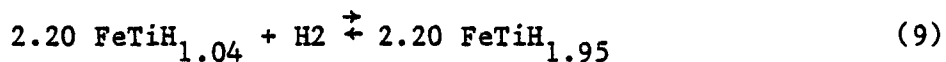
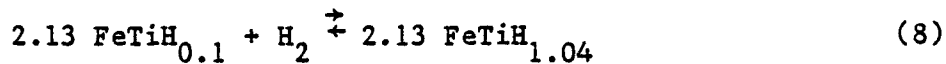
It should be mentioned that disproportionation reactions can be useful tools for the determination of metallurgical thermodynamic data. For example, knowing  $\Delta G_{f298}^{\circ}$  for  $Mg_2Cu$ ,  $MgH_2$  and the overall  $\Delta G^{\circ}$  for reaction (5), the calculated  $\Delta G_{f298}^{\circ}$  for  $MgCu_2$  is  $-8.6$  kcal, which is in good agreement with the literature value of  $-8.15$  kcal.<sup>15</sup>

## II.B Iron-Titanium Alloys

The iron-titanium-hydrogen and related systems presently constitute the most promising candidates for application as hydrogen storage media. Their advantage is derived from the low cost and high abundance of the raw material from which the starting alloys can be produced.

The iron-titanium phase diagram exhibits two stable intermetallic compounds, FeTi and  $Fe_2Ti$ .<sup>12</sup> The latter does not react with hydrogen between 78 and 573 K and between 78 and 298 K at hydrogen pressures of 65 and 540 atm, respectively. FeTi reacts directly and reversibly with hydrogen to form two tern-

ary hydrides<sup>16</sup> whose properties are listed in Table 3. The reactions which take place stepwise can be written (starting with the hydrogen saturated metal) as follows:



The products of the reactions are gray metal-like solids with essentially the same appearance as the initial alloy.

The alloy is not pulverized by hydriding, although the hydride phases are very brittle and exhibit extensive microcracking. After the initial hydriding-dehydriding cycle the alloy surface area typically ranges from 0.2-0.5m<sup>2</sup>/g. Exposure of these materials to air tends to deactivate them and, even though both hydrides have dissociation pressures appreciably above 1 atm at 25°C, they will decompose (i.e., evolve hydrogen) only very slowly in air, if at all. Once exposed to air they may be reactivated by repeating the initial activation procedure. This deactivation phenomenon can be used to advantage as it permits one to handle a deactivated sample in open air without decomposition; both X-ray and neutron diffraction measurements and density determinations have been made using such deactivated samples. A family of dissociation pressure-composition isotherms for the FeTi-H system is shown in Figure 4; also shown is an absorption isotherm which illustrates the rather large hysteresis effect.

The rate of decomposition of iron titanium hydride at near room temperature has been reported.<sup>13</sup> The reaction is very rapid and special care must be taken to assure isothermal conditions. The decomposition of FeTiH<sub>1.0</sub> obeys first order kinetics and the rate constants are listed below.

Table 4. Decomposition of FeTiH<sub>1.0</sub>

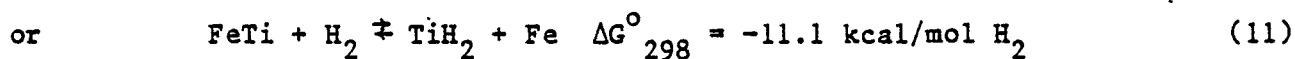
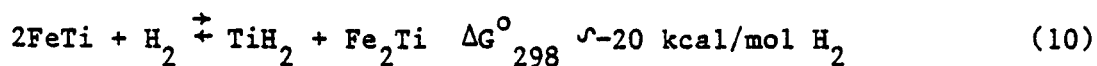
| <u>Temp. °C</u> | <u>First-Order<br/>Rate Constant</u>     |
|-----------------|--|
| 0               | 1.5 x 10 <sup>-2</sup> sec <sup>-1</sup> |
| 19              | 4.0 x 10 <sup>-2</sup> sec <sup>-1</sup> |
| 29              | 5.9 x 10 <sup>-2</sup> sec <sup>-1</sup> |

Lindner<sup>17</sup> has used these data to construct a model in which diffusion of hydrogen out of the hydride phase is the rate determining step.

This system is quite sensitive to changes in composition or the presence of contaminants. Its effective storage capacity is adversely affected by the presence of oxygen which is apparently due to the formation of an inactive oxide phase of the approximately composition Fe<sub>7</sub>Ti<sub>10</sub>O<sub>3</sub>.<sup>18</sup>

As with many other alloy hydrides, the P-C-T properties of the system can be modified by the addition or substitution of another transition metal component.<sup>19</sup> One particular ternary alloy is of interest, TiFe<sub>x</sub>Mn<sub>y</sub>.<sup>20</sup> With small amounts of Mn the activation of the alloy can be carried out at room temperature, whereas FeTi requires outgassing at √300°C, as illustrated in Table 5. It should also be noted that the p-C isotherms (Figure 5) for a low Mn materials are only slightly distorted relative to pure FeTiH<sub>x</sub>, but the hysteresis effect is reduced significantly.<sup>20</sup>

Titanium forms a rather stable binary hydride ( $\Delta G_{f298}^{\circ} = -20$  kcal) and the disproportionation of known ternary hydrides having a Ti content  $\geq 50$  atom percent to form TiH<sub>2</sub> is always thermodynamically favorable at low temperatures; a tendency which is enhanced if a lower Ti intermetallic compound exists in the alloy system in question. Iron titanium hydride is no exception and, as shown below, is a thermodynamically metastable phase.



Of course, the equilibrium pressures corresponding to the above systems are too low for energy storage applications. Despite the large thermodynamic driving force, reactions (10) and (11) will not occur at low temperatures to any appreciable extent (there may be, however, surface segregation as noted below). This was demonstrated in several long-term experiments in which  $\text{FeTiH}_x$  was subjected to up to 30,000 hydriding-dehydriding cycles with the temperature ranging from  $0^\circ\text{-}100^\circ\text{C}$ .<sup>21</sup> There was no deterioration in the behavior of the system as measured by the constancy of the  $\Delta\text{H}/\text{Ti}$  in each cycle, nor was there any evidence of the formation of  $\text{TiH}_2$ ,  $\text{TiFe}_2$  or Fe as determined by X-ray analysis. However, there was a large change in magnetic susceptibility, an effect which was previously reported by Hempelmann and Wicke,<sup>22</sup> who suggested the increase is due to the formation of small Fe clusters. Schlapbach et al.<sup>23</sup> have attributed this change in magnetic properties to surface segregation, thus forming Ti and Fe clusters and have produced direct experimental evidence of their existence. They have also noted similar surface segregation effects in  $\text{LaNi}_5\text{-H}$  systems.<sup>24</sup>

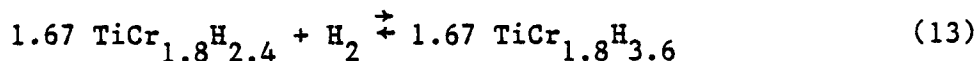
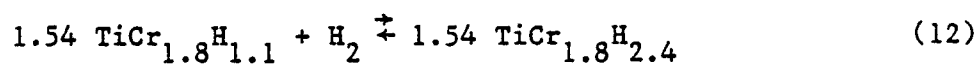
While no significant disproportionation of bulk FeTi has been noted, even at elevated temperatures ( $\approx 450^\circ$ ), other Ti intermetallic compounds which form ternary hydrides at room temperature have been observed to do so. Yamanaka et al.<sup>6</sup> report the following alloys disproportionate, at the indicated temperature, in the presence of hydrogen;  $\text{TiNi}$  ( $500^\circ\text{C}$ ),  $\text{Ti}_2\text{Ni}$  ( $250^\circ\text{C}$ ),  $\text{TiCu}_3$  ( $500^\circ\text{C}$ ),  $\text{TiCu}$  ( $200^\circ\text{C}$ ) and  $\text{Ti}_2\text{Cu}$  ( $200^\circ\text{C}$ ). Reilly has also noted the disproportionation of  $\text{Ti}_2\text{Co}$  at  $>350^\circ\text{C}$ .<sup>21</sup>

Thompson et al. have recently defined the structures of the  $\beta^{25}$  and  $\gamma^{26}$  phases of iron titanium deuteride using neutron diffraction techniques. The  $\beta$  phase is orthorhombic with  $a = 2.956 \text{ \AA}$ ,  $b = 4.543 \text{ \AA}$ , and  $c = 4.388 \text{ \AA}$ ; the deuterium atoms are ordered on octahedral sites with two nearest neighbor iron atoms; Shlapbach et al. confirm the  $\beta$  phase structure.<sup>27</sup> The  $\gamma$  phase is monoclinic, space group  $Pc/m$  with  $a = c = 4.7044 \text{ \AA}$ ,  $b = 2.8301 \text{ \AA}$ , and  $\beta = 96.57^\circ$ ; the unit cell contains two formula units and the deuterium atoms are ordered on octahedral sites. There is no evidence of exchange or clustering of iron and titanium atoms in the bulk matrix.

### III.B Ti-Cr Alloys

The Ti-Cr alloy system exhibits one intermetallic compound  $TiCr_2$ , of which there are two temperature-dependent allotropes.<sup>28</sup> Both are Laves phases, the low temperature form having the cubic  $MgCu_2$  (C15) structure, while the high temperature form has the hexagonal  $MgZn_2$  (C14) structure. Both forms will react with hydrogen to form hydride phases, but only the  $TiCr_2$  (C15)-H system has been defined.<sup>29</sup>

At room temperature the limits of homogeneity for the C15 phase have compositions corresponding to  $TiCr_{1.71}$ - $TiCr_{1.92}$ . At  $-78^\circ C$  and 60 atm pressure, the hydrogen saturated C15 phase will react sequentially with hydrogen to form two distinct hydride phases:



The product of reaction (13) represents the highest hydrogen content of the solid phase observed to date.

A P-C-T diagram for the system is shown in Figure 6. Thermodynamic values derived from these data are given in Table 6. It should be mentioned that in order to obtain single phase C15 samples, a rather extensive and complex annealing treatment was required. If mixed phase samples are used, P-C-T data are distorted. This system is notable for the all but nonexistent hysteresis effect.

At room temperature, only one hydride phase exists having a composition range extending from  $\text{TiCr}_{1.8}\text{Cr}_{2.1}$  to  $\text{TiCr}_{1.8}\text{H}_{3.6}$ . This phase is orthorhombic with the lattice parameters varying slightly with hydrogen content.

Whereas the theory of Reversed Stability would predict the formation of stable hydrides from  $\text{TiCr}_2$  they are, in fact, very unstable, even to the point of limited utility for practical applications. However, as with other alloy hydrides, it is possible to modify their properties by composition changes. An example of such modification is shown in Figure 7, in which Mn has been substituted in part for Cr.<sup>30</sup>

Finally, as would be expected, both ternary hydrides are metastable with respect to formation of  $\text{TiH}_2$  and Cr. However, upon short term exposure of  $\text{TiCr}_{1.8}$  (C15) to hydrogen at  $450^\circ\text{C}$ , there was no indication of the formation of any  $\text{TiH}_2$  and/or Cr.

#### IV.B Rare Earth Alloys

Van Vucht et al.<sup>31</sup> found that a number of intermetallic compounds of the  $\text{AB}_5$  type (where A is a rare earth metal and B is Ni or Co) will react directly and reversibly with hydrogen to form a ternary metal hydride. The archetype and most thoroughly investigated of these alloys is  $\text{LaNi}_5$ . It will react rapidly with hydrogen (even in ingot form) at room temperature at a pressure of several tens of atmospheres. A pressure-composition diagram for this system is shown in



Figure 8. It is notable that the hysteresis effect is relatively small, particularly when compared to other low temperature systems with a large and distinct miscibility gap. The reaction may be written as follows:



A particular advantage of the  $\text{AB}_5$  hydride family is that the properties of the alloy-hydrogen system can be varied almost at will by substituting in whole or in part other metals for lanthanum and Ni. For example, mischmetal, which is a mixture of rare earth metals, when substituted for La forms a hydride having about the same hydrogen content but is much more unstable.<sup>13</sup>

Lundin et al.<sup>8</sup> have carried out a systematic study of such substitutional alloys and have correlated the free energy of formation (plateau region) with the change of the interstitial hole size caused by the substituted metal component. Plots of the variation of  $\Delta G$  vs. the radius of the interstitial hole for several homologous  $\text{AB}_5$  alloy series are shown in Figure 9. Gruen et al.<sup>9</sup> have taken a similar approach, but use the change in lattice parameter rather than interstitial hole size as the measure. They were concerned in formulating an alloy hydride which would have optimum P-T-C properties for a heat pump application. Sandrock<sup>32</sup> has carried out similar investigations but with the objective of producing low cost hydrogen storage alloys rather than a unique alloy-hydrogen system having optimized properties for a particular application.

### C. APPLICATIONS OF METAL HYDRIDES

The convenient storage of hydrogen is tantamount to the convenient storage of energy. Thus, it is not surprising that most attention for the practical application of metal hydrides has focused on their potential as energy storage media. However, there are other possible applications, some of which are already in practice, albeit on a small scale.

## I.C Criteria

In order to serve as a practical energy or hydrogen storage medium, a metal hydride must satisfy a number of criteria. Perhaps the most important is that it be easily formed and decomposed. Obviously, very stable hydrides (e.g.,  $ZrH_2$ ,  $TiH_2$ , etc.) are not suitable and we are limited to those hydrides which will decompose at relatively low temperatures ( $\leq 300^\circ C$ ). A further important criterion concerns their heat of decomposition, which even in the case of unstable hydrides, is substantial. In fact, if the use of metal hydrides as energy storage media is to be feasible, the heat of decomposition must be supplied from the waste heat of the energy converter with which it is coupled. Thus, there must be a match between the energy converter and the pressure-temperature characteristics of the metal hydride. For example, it appears possible to use  $MgH_2$  as a source of hydrogen fuel for an internal combustion engine, using the high temperature exhaust heat to provide most, if not all, of the heat of decomposition. However, it would not be feasible to couple it to a fuel cell that rejects heat at  $150^\circ C$ . A flow diagram is shown in Figure 10 which illustrates this relationship. In this case, unstable iron titanium hydride is used as the hydrogen fuel storage compound. The heat of decomposition is supplied from the waste heat of the converter by circulating its coolant through a heat exchanger in contact with the metal hydride. The heat must be supplied at a rate sufficient to satisfy the fuel demand of the converter. Thus, if the reservoir temperature can be maintained at  $25^\circ C$  by the waste heat, the hydride is readily capable of delivering  $H_2$  fuel continuously at high flow rates and at pressures in excess of one atmosphere. If the heat supply is insufficient, the latent heat of decomposition will be supplied from the sensible heat of the surroundings, consequently, the bed will progressively cool

and the  $H_2$  flow will decrease until a balance is struck between the decomposition rate and the heat input. When the bed is exhausted, it can be regenerated by following the opposite procedure, i.e., it is contacted with hydrogen at a pressure substantially above the dissociation pressure, making due allowance for hysteresis, and a coolant is circulated through the bed to remove the heat of reaction.

Other criteria involve cost, safety, suitable reaction rates, weight and chemical and physical stability. Their relative importance will depend in some degree upon the specific application. For example, in stationary storage applications weight is not a critical parameter, whereas for automotive applications it is very important. At this time there are a number of candidate metal-hydrogen systems. Their pertinent properties are listed in Table 8.

#### II.C Automotive

The use of catalyzed  $MgH_2$  as an automotive hydrogen fuel storage compound was suggested by Hoffman et al.<sup>33</sup> in 1969. It was proposed that the exhaust heat of the engine be used to supply the heat of decomposition. However, despite the high hydrogen content of this material, there are two problems which have so far hindered its development as a practical storage compound. The most severe problem is that the heat of decomposition must be supplied at a temperature of 300°C or above. A less serious difficulty is that the rate of generation of usable waste heat does not quite match the rate at which  $MgH_2$  must decompose in order to satisfy engine fuel demand. This shortfall can be accommodated by either burning a portion of the stored hydrogen to supplement the waste heat or to use an additional fuel storage bed of a less stable hydride. Indeed, this latter option has already been adopted as we will note below.

Even though  $\text{FeTiH}_x$  stores substantially less hydrogen per unit weight than Mg alloy hydrides, it has been the focus of most attention for mobile applications because of its convenient temperature-pressure properties. Of course, weight comparisons are relative and, by this measure, FeTi alloy hydrides are quite competitive with another alternative automotive power source, i.e., electric batteries as shown in Table 9. Indeed the virtues of  $\text{FeTiH}_x$  have been recognized and a number of experimental hydrogen powered vehicles have been built using it as the storage medium; these are listed in Table 10. For a detailed description of the vehicles and their associated performance the reader is referred to the reference cited.

Perhaps the most recent advance in this area is the use of a dual bed storage system; one consisting of a FeTi alloy hydride and the other of a Mg-Ni alloy hydride.<sup>34</sup> There is a distinct advantage to such a system; it is a compromise which should eventually result in the most optimum mobile storage system. The reason for this is the waste heat in conventional automotive engines is not generated at a sufficient rate or quality to decompose the Mg alloy hydride at the rate required to satisfy engine fuel demand. The shortfall is made up by generating some hydrogen from the FeTi alloy bed using plentiful, low quality, waste heat. The compromise consists of using both beds in such a way that sufficient high quality heat is available for the Mg bed and the remaining heat is used for the FeTi bed. Such a system appears to have the potential of storing up to 5 wt %  $\text{H}_2$ .

Nevertheless, despite its promise, complete substitution of hydrogen for gasoline can only be considered as a long-term option because of the massive investment which would be required for its production and distribution. However, there are certain short-term applications where such constraints would not

operate. One particularly attractive possibility would involve hydrogen-powered fleet vehicles serviced by central garages. Such vehicles, because of the almost zero pollution characteristics of hydrogen fuel, would be very desirable in congested urban or industrialized areas. In fact, the two buses listed in table 10 were commissioned by local government agencies for this very reason. Opportunities also exist in the area of low pollution industrial and mine vehicles. In these latter types, the weight disadvantage of the hydride (vs. liquid fuel) is not significant because such vehicles usually carry a heavy ballast, in fact, many are battery powered because of the low pollution imperative. A recent study by Lynch and Snape<sup>35</sup> of in-plant, industrial, vehicles contends that even current designs for hydrogen fueled fork lift trucks are competitive, in terms of overall yearly cost, with conventional designs.

It is also important to recognize that it may not be necessary to burn hydrogen exclusively in order to realize very substantial environmental and fuel (hydrocarbon) economy benefits. In the United States, 95% of all private automobile trips are less than 48 km (30 miles) in length and these trips account for about 60% of all vehicle miles.<sup>37</sup> In view of these data, Reilly et al.<sup>36</sup> proposed a vehicle capable of using both hydrogen and gasoline alternately which would be a desirable compromise for the intermediate term (Figure 11). An alternate design would incorporate the ability of burning gasoline and hydrogen simultaneously. Hoehn et al.<sup>38</sup> have shown that the inclusion of hydrogen into the gasoline feed stream increases the thermal efficiency of fuel mixture substantially when compared to gasoline alone. Recently, Buchner and Säufferer have reported the conversion of a passenger vehicle to such hybrid operation; the vehicle is currently undergoing tests.<sup>34</sup>

### III.C Utility Load Leveling

The storage of electrical energy through the production, storage and reconversion of hydrogen is of interest as a load leveling technique for electric utilities.<sup>39</sup> The entire process has been demonstrated on an engineering scale by Public Service Electric & Gas Company of New Jersey (PSE&G) and a flow diagram of this system is shown in Figure 12. Hydrogen is produced electrolytically, compressed from 5 to 35 atm and stored as iron titanium hydride. Subsequently, the hydride is decomposed to provide hydrogen fuel to a fuel cell. In practice hydrogen would be produced using off-peak power, stored and then reconverted to electricity to satisfy on-peak loads. The hydrogen storage reservoir contained 400 kg of a ferrotitanium alloy and had an effective storage capacity of 6.4 kg of hydrogen. It was designed to operate through a complete sorption-desorption cycle once a day. In the sorption mode, heat was removed by circulating cold water ( 17 C) through an internal heat exchanger; for the reverse, desorption reaction, heat was supplied by circulating 45 C water through the exchanger. The system has undergone about 60 full sorption-desorption cycles without difficulty.<sup>40</sup>

While the use of iron titanium hydride in such a system as described above has been proven feasible, it is also apparent that its properties are not ideal for full scale peak shaving systems. The reference design<sup>41</sup> of a 26 mw storage system that has been recently proposed specifies the use of a fuel cell system which rejects heat at a temperature of 160°C. The cooling water temperature is specified as 30°C. If pure FeTi were used as the storage compound, a charging pressure considerably in excess of 35 atm would be required in order to store as much hydrogen as the PSE&G unit which had cooling water available at 17°C. Further, no advantage could be taken of the high quality heat which is rejected by

the fuel cell because of the high dissociation pressure of  $\text{FeTiH}_x$ . Obviously, a more stable hydride could be used to good advantage in this particular instance and it was proposed that binary FeTi be replaced with a ternary alloy having a composition corresponding to  $\text{TiFe}_{.7}\text{Mn}_{.2}$ . A comparison of its predicted performance vs. that of FeTi is given in Table 11.

#### IV.C Thermal Storage

The first heat storage system involving a metal hydride was proposed by Winsche.<sup>42</sup> Heat derived from a low level radioactive isotope was used to slowly decompose  $\text{MgH}_2$  (catalyzed) over a relatively long period of time. During this "charging" period the hydrogen product was stored as iron titanium hydride. The heat of formation of the latter was rejected to the surroundings. In the "discharge" mode the reactions were reversed, iron titanium hydride was decomposed using ambient heat and  $\text{MgH}_2$  was regenerated at an elevated temperature ( $>300^\circ\text{C}$ ). The heat evolved in this step was used to produce high quality steam which performed work.

A scheme coupling solar energy with a metal hydride thermal storage system was suggested by Libowitz.<sup>43</sup> Solar heat is used to decompose  $\text{FeTiH}_x$ , or a similar hydride, at an elevated temperature and the hydrogen stored as a pressurized gas. In order to release the stored energy, the pressurized hydrogen gas is permitted to react with the previously dehydrided alloy at a lower temperature. Unfortunately, at the present time it does not appear, as later pointed out by Libowitz<sup>(44)</sup>, that the storage of low quality heat (e.g., solar heat) using unstable hydrides, is economically feasible. This is a consequence of cost of the alloy per unit hydrogen stored and the low heat of formation. However, the assessment is not so bleak where the storage of high quality heat is concerned. In this case, magnesium can be used which is relatively cheap and

has an effective hydrogen storage capacity several times that of any unstable alloy hydride (Table 8). It is rather interesting that in this context the relatively high heat of formation and stability of  $MgH_2$  are assets rather than liabilities. Thus, a thermal storage process has been proposed, using  $MgH_2$ , for electric utilities.<sup>21</sup> The thermal charging step consists of decomposing  $MgH_2$  at  $\sim 335^\circ C$ , storing the hydrogen as a FeTi alloy hydride. In the thermal discharge step the low temperature hydride is decomposed using waste heat ( $< 80^\circ C$ ) and evolved hydrogen is recombined with Mg at  $\sim 335^\circ C$ . The heat produced is used to generate high pressure steam. It is worthwhile noting that in such a thermal storage system only in the final step is thermal energy converted to electricity and the overall efficiency is likely to be in the 25-33% range which compares quite favorably to other energy storage systems proposed for utilities.

#### V.C Heat Pumps

The rather large latent heat effects of metal-hydrogen systems can be exploited to design novel heat pump cycles. In essence, the device consists of two metal hydride beds, an evaporator bed and a condenser bed as shown in Figure 14. Gruen et al.<sup>45</sup> have designed and built a demonstration facility (HYCSOS) to test various alloy hydride and bed configurations. Initial designs incorporated a heat storage capability which was later eliminated because of its high cost. Present designs specify two different  $AB_5$  alloy hydride beds having matched pressure-temperature characteristics to give optimum performance. The beds are cycled very rapidly to reduce alloy inventory to a minimum. A mechanical compressor is not required.

Most recently Alefeld<sup>46</sup> has proposed a heat pump topping cycle for power generation using a high temperature Mg alloy hydride and low temperature ferrotitanium or  $AB_5$  alloy hydride. The author envisages an increase in power



generation efficiency from 37 to 49%. The cycle is rather complicated and for a full discussion the reader is referred to the references cited.

#### VI.C Hydride Compressors

The hydriding and dehydriding reactions of a number of unstable metal-hydrogen systems are rapid enough to consider their use as hydrogen compressors or pumps. The pumping action is derived from the alternate decomposition and reformation of a metal hydride using low grade heat and a heat sink to provide the driving force. The first such pump using an unstable hydride was built in 1971<sup>47</sup> for laboratory use and is still in operation. The pumping action was obtained by the alternate decomposition and reformation of  $VH_2$  using hot ( $50^\circ C$ ) and cold ( $18^\circ C$ ) water. A more sophisticated and higher capacity compressor has recently been built using  $LaNi_5H_x$  and its operation is described by Van Mal.<sup>48</sup>

An interesting variant has been suggested by Powell et al.<sup>49</sup> who are concerned with highly efficient power conversion systems. It is based on using a low temperature heat source in combination with a high temperature heat source in a close Brayton cycle where hot compressed gas is expanded through a turbine. The novel feature of the system is the use of an unstable hydride and low temperature heat to effect the compression of the gas, thereby eliminating mechanical compressor work and substantially increasing the efficiency of the use of the high temperature heat.

#### VII.C Isotope Separation

In many cases there may be quite large differences in thermodynamic stability between the protides, deuterides and tritides of a given metal or alloy. Wiswall and Reilly<sup>50</sup> have noted that  $VD_2$  is appreciably more stable than  $VH_2$  at or near room temperature and measured the separation factor,  $\alpha$ , for hydrogen-tritium mixtures in vanadium and several alloy hydrides. Recently

Tanaka et al.<sup>51</sup> have determined  $\alpha_{H-T}$  for a number of Ti intermetallic alloy hydrides which are listed in Table 12. Wiswall et al.<sup>52</sup> have recently proposed a chromatographic separation process for hydrogen isotope separation and recovery.

#### VIII.C Hydrogen Purification

It is possible to conceive of the use of metal hydride former to selectively extract hydrogen from mixed gas streams, e.g., reformer gas. Unfortunately, all known hydride formers are easily poisoned by  $O_2$ , CO,  $H_2O$ , etc. There are, however, some systems that are relatively resistant; for example, Cholera and Gidaspow<sup>53</sup> have used a Fe-Ti-Ni alloy to extract hydrogen from a methane-hydrogen mixture. Reilly and Wiswall have used  $AB_5$  alloys to extract hydrogen from simulated reformer gas mixtures containing small amounts of CO.<sup>54</sup>

In the latter case it was noted that  $LaNi_5$  reacted readily in  $H_2-CO_2$  mixtures; however, the presence of 1% CO completely destroyed its activity toward hydrogen at 25°C. A ternary alloy  $LaNi_{5-x}Cu_x$  seemed to be more tolerant and did react in gas mixtures containing up to 4% CO, although its activity and/or capacity was drastically reduced.

#### IX.C Process and Laboratory Storage

The current annual production of hydrogen is  $\sim 4.5 \times 10^7$  metric tons. It is primarily used in the chemical process industries for the production of a myriad of products ranging from plastics to fertilizers. It is likely that convenient storage of hydrogen would be very desirable in many processes to provide surge capacity, reserve supplies, high purity hydrogen, etc.

Iron titanium hydride is currently being used in our laboratory to provide a source of high purity hydrogen and deuterium at pressures up to 60 atm.<sup>55</sup>

Wenzl and Klatt<sup>56</sup> have described the performance of commercially available cylinders storing up to seven Kg of  $\text{FeTiH}_x$ . They are capable of supplying hydrogen at a purity of 99.9999% after being charged with hydrogen of 99.9% purity. In the United States, cylinders of  $\text{FeTiH}_x$  are commercially available from the Billings Energy Corporation, Provo, Utah.

#### X.C Safety

All chemical fuels are inherently hazardous. The extent of the hazard depends upon the fuel properties, e.g., coal is much less hazardous than liquefied natural gas, the properties of liquid hydrogen would forbid its use as an ordinary, common, fuel even though in high technology applications large amounts have been handled without incident. On the other hand, low pressure hydrogen gas is relatively safe; in fact, "town gas," which was a major fuel in many large cities in the past, contained about 50 volume % hydrogen. With respect to metal hydrides, a number of safety-related studies have been carried out.<sup>57-61</sup> Most were concerned with the ignition of these materials in air and these results are summarized in Table 13. In addition to these standard tests, Woolley<sup>62</sup> reports several involving the catastrophic rupture of reservoirs containing iron titanium hydride by armor piercing incendiary bullets. Only momentary ignition occurred whereas the results of a similar test in which gasoline was substituted for  $\text{FeTiH}_x$  resulted in a rather spectacular conflagration. In view of this latter experiment, it may be concluded that  $\text{FeTiH}_x$  is inherently less hazardous than most common, volatile fuels currently widely used.

ACKNOWLEDGMENT

This review was written under the auspices of the Basic Energy Sciences Division of the U.S. Department of Energy, Washington, D.C., under Contract #EY76-C-02-0016.

## REFERENCES

1. For a general review of metal hydride chemistry, see W. M. Mueller, J. P. Blackledge, and G. C. Libowitz, (1968) Metal Hydrides, Academic Press, New York and London; also G. Alefeld and J. Völkl (eds.) Topics in Applied Physics; Hydrogen in Metals Vols. I and II Springer-Verlag, Berlin-Heidelberg-New York, 1978.
2. J. J. Reilly and R. H. Wiswall, Annual Report Nuclear Engineering Dept., p. 36, U.S.A.E.C., BNL-50023(S-69), Brookhaven National Laboratory, Upton, N.Y., 1966.
3. H. H. Van Mal, Stability of ternary hydrides and some applications, Thesis, Technische Hogeschool, Delft, 1976.
4. A. R. Miedema, R. Boom and F. R. DeBoer, J. Less-Common Metals 41, 283 1975.
5. H. H. Van Mal, K. H. J. Bushow and A. R. Miedema, J. Less-Common Metals 35, 65, 1974.
6. K. Yamanaka, H. Saito and M. Someno, Nippon Kagaku Kaishi (J. Chem. Soc. Japan) 8, 1256, 1975.
7. C. Wagner Acta Met. 19, 843, 1971.
8. C. E. Lundin, F. E. Lynch and C. B. Magee, J. Less-Common Metals, 56, 19-37, 1977.
9. D. M. Gruen, M. H. Mendelsohn and Austin E. Dwight, Advances in Chemistry Series 167 Transition Metal Hydrides, R. Bau Editor, American Chemical Society Wash. D.C., 1978, pp 327-341.
10. F. H. Ellinger, C. E. Holley, B. B. McInteer, D. Ponone, R. M. Potter, E. Starityky and W. H. Zochariosen, J. Am. Chem. Soc. 2647, 77, 1955.
11. J. J. Reilly and R. H. Wiswall, Jr., Inorg. Chem. 7, 2254, 1968.

12. M. Hansen, Constitution of Binary Alloys, 2nd Edition, McGraw-Hill, New York, 1958.
13. J. J. Reilly, "Hydrogen: Its Technology and Implications, Vol. II. Transmission and Storage of Hydrogen" Cox, K. E. and Williamson, K. D., Eds., Chap. 2, CRC Press, Cleveland, Ohio, 1977.
14. J. J. Reilly and R. H. Wiswall, Jr., Inorg. Chem. 6, 2220, 1967.
15. R. Hultgren, P. D. Desai, P. T. Hawkins, M. Gleiser and K. K. Kelly, Selected Values of the Thermodynamic Properties of Binary Alloys, American Society for Metals, Metals Park, Ohio, 1973.
16. J. J. Reilly and R. H. Wiswall, Jr., Inorg. Chem. 13, 218, 1974.
17. D. L. Lindner Inorg. Chem. 17, 3721, 1978.
18. G. Sandrock, J. R. Johnson and J. J. Reilly, Metallurgical considerations in the production and use of FeTi alloys for hydrogen storage, Proceedings 11th Intersociety Energy Conversion and Engineering Conf., Lake Tahoe, Stateline, Nevada, American Institute of Chemical Engineers, N.Y., 1976.
19. J. J. Reilly and J. R. Johnson, Titanium alloy hydrides and their applications, Proceedings 1st World Hydrogen Energy Conf., Miami Beach, Fla., Univ. of Miami, 1976.
20. J. R. Johnson and J. J. Reilly, The Use of Manganese Substituted Ferrotitanium Alloys for Energy Storage, Proceedings of the Int. Conf. on Alternative Energy Sources, Miami Beach, Fla., 1977.
21. J. J. Reilly, Proceedings Int. Symp. on Hydrides for Energy Storage, Geilo, Norway, 1977, A. F. Andresen and A. Maeland, eds., pp. 301-322, Pergamon Press, London, 1978.
22. R. Hempelmann and E. Wicke, Ber. Bunsenges. physik. Chem. BD81, Nr. 4, 1977.

23. L. Schlapbach, A. Seeler and F. Stucki, Mat. Res. Bull. 13, 697, 1978.
24. H. C. Sergmann, L. Schlapbach and C. R. Brundle, Phys. Rev. Letters 40, 972, 1978.
25. P. Thompson, M. A. Pick, F. Reidinger, L. M. Corliss, J. M. Hastings and J. J. Reilly, J. Phys. F: Metal Physics, L 75-80, 1978.
26. P. Thompson, J. J. Reilly, F. Reidinger, J. M. Hastings and L. M. Corliss, J. Phys. F: Metal Physics, in press.
27. P. Fischer, W. Hälg, L. Schlapbach, F. Stucki, and A. F. Andresen Mat. Res. Bull. 13, 931-46, 1978.
28. P. A. Farrar and H. Marzolin, Trans. Met. Soc. AIME 227, 1342, 1963.
29. J. R. Johnson and J. J. Reilly, Inorg. Chem. 17, 3103, 1978.
30. J. R. Johnson, Unpublished data, Brookhaven National Lab., Upton, N.Y., 1979.
31. J. H. N. van Vucht, F. A. Kuijpers, and H. C. A. M. Bruning, Philips Res. Reports 25, 133, 1970.
32. G. D. Sandrock, Proceedings 2nd World Hydrogen Energy Conf. Zurich 1978, T. N. Veziroglu and W. Siefritz (eds.), pp. 1625-1657, Pergamon Press, London, 1978.
33. K. Hoffman, W. E. Winsche, R. H. Wiswall, J. J. Reilly, T. V. Sheehan, and C. H. Waide, Metal hydrides as a source of fuel for vehicular propulsion, Int. Automotive Eng. Congress, Detroit, S.A.E. 690232, 1969.
34. H. Buchner and H. Säufferer, Proceedings 2nd World Hydrogen Energy Conf. Zurich 1978, T. N. Veziroglu and W. Siefritz (ed.), pp. 1749-1793 Pergamon Press, London, 1978.
35. F. Lynch and E. Snape, *ibid.*

36. J. J. Reilly, K. C. Hoffman, G. Strickland, R. H. Wiswall, Iron titanium hydride as a source of hydrogen fuel for stationary and automotive applications, 26th Annual Proceedings Power Sources Conf., Atlantic City, New Jersey, 1974.
37. R. V. Ayres and R. P. McKenna, Alternatives to the Internal Combustion Engine, p. 10, Johns Hopkins University Press, Baltimore, Maryland, 1972.
38. F. W. Hoehn, F. W. Barsley and M. W. Dowdy, Proceedings 10th Intersociety Energy Conversion Engineering Conf., pp. 1156-1165, Inst. of Electrical and Electronic Engineers, N.Y., 1975.
39. J. M. Burger, P. A. Lewis, R. J. Isler, F. J. Salzano and J. M. King, Energy storage for utilities via hydrogen systems, Proceedings 9th Intersociety Energy Conversion Eng. Conf., San Francisco, Calif., American Society of Mechanical Engineers, N.Y., 1974.
40. C. R. Guerra, Public Service Electric and Gas Corp., Newark, New Jersey, Private communication.
41. A. Beaufrere, F. J. Salzano, R. Isler, and W. Yu, Hydrogen storage via FeTi for a 26 MW peaking electric plant, Proceedings 1st World Hydrogen Energy Conf., Miami Beach, Fla., Univ. of Miami, 1976.
42. W. Winsche, Intermittent Power Source, U.S. Patent 3,504,494 (April 7, 1970).
43. G. G. Libowitz, Metal hydrides for thermal energy storage, Proceedings 9th Intersociety Conversion Energy Conf., San Francisco, Calif., American Society of Mechanical Engineers, N.Y., 1974.
44. G. G. Libowitz and Z. Blank, An evaluation of the use of metal hydrides for solar thermal energy storage, Proceedings 11th Intersociety Energy Con-



- version Eng. Conf., Stateline, Nevada, American Institute of Chemical Engineers, N.Y., 1976.
45. D. M. Gruen, R. L. McBeth, M. Mendelsohn, J.M. Nixon, F. Schreiner, and I. Sheft, Hycsos: A solar heating, cooling and energy conversion system based on metal hydrides, Ibid.
46. G. Alefeld in Hydrogen in Metals II, pp. 2-9, see ref. 1 for complete citation.
47. J. J. Reilly, A. Holtz, and R. H. Wiswall, Jr., Rev. Sci. Instrum. 42, 10, 1495, 1971.
48. H. H. Van Mal, Proc. Int. Symp. on Hydrides for Energy Storage, Geilo Norway, 1977 A. F. Andresen and A. J. Maeland (eds), pp. 251-261, Pergamon Press, London, 1978.
49. J. R. Powell, F. J. Salzano, Wen-Shi Yu, J. S. Milau, A high efficiency power cycle using metal hydride compressors USERDA Report, BNL 50447, Brookhaven National Laboratory, Upton, New York, 1975.
50. R. H. Wiswall, Jr. and J. J. Reilly Inorg. Chem. 11, 1691, 1972.
51. J. Tanaka, R. H. Wiswall and J. J. Reilly, Inorg. Chem. 17, 498 (1978).
52. R. H. Wiswall, J. Reilly, F. Block and E. Wirsing, Hydrogen Isotope Exchange in Metal Hydride Columns, BNL 50755, Brookhaven National Laboratory, Upton, N.Y., 1978.
53. V. Cholera and D. Gidaspow "Hydrogen Separation and Production from Coal-Derived Gases Using  $\text{Fe}_x\text{TiNi}_{i-x}$ " Proc 12th Intersociety Energy Conversion Engineering Conf. 1977.
54. R. H. Wiswall in Hydrogen in Metals II, pp. 201-242, for complete citation see ref. 1.

55. R. H. Wiswall and J. J. Reilly, Method of Storing Hydrogen U.S. Patent, 3 516, 263 (June 23, 1970)
56. H. Wenzl and K. H. Klatt Proc. Int. Symp. on Hydrides for Energy Storage Gielo Norway 1977, pp. 323-329, A. F. Andresen and A. Maeland, (eds), Pergamon Press, London, 1978.
57. T. R. P. Gibb, Jr. and C. E. Messer, A survey report on lithium hydride, USAEC Report, NYO-3957, Tufts College, 1954.
58. M. E. Lee, Other saline hydrides, USAEC Report, NEPA-669, Fairchild Engine and Airplane Corp. (1948).
59. I. Hartmann, The explosibility of titanium, zirconium, thorium, uranium, and their hydrides, USAEC Report NYO-1562, Bureau of Mines, 1951.
60. C. E. Lundin and F. E. Lynch, Safety characteristics of FeTi hydride, Proceedings Intersociety Energy Conversion and Eng. Conf., Univ. of Delaware 1975, Institute of Electrical and Electronic Engineers, N.Y., 1975.
61. C. E. Lundin and R. W. Sullivan, The safety characteristics of LaNi<sup>5</sup> hydrides, Proc. THEME Conf., Miami Beach, Univ. of Miami, 1974.
62. R. L. Woolley, Performance of a hydrogen powered transit vehicle, Proceedings 11th Intersociety Conversion Eng. Conf., Stateline, Nevada, American Institute of Chemical Engineers, N.Y., 1976.
63. A. R. Landgrebe, Secondary batteries for electric vehicles, Proceedings of the Symp. and Workshop on Adv. Battery Research and Design, p. A-24, USERDA Report, ANL-76-8, March 1976.
64. V. R. Anderson, Proceedings 2nd World Hydrogen Energy Conf., Zurich, Switzerland, T. N. Veziroglu and W. Seifritz, eds. Pergamon Press, London, pp. 1879-1901, 1978.
65. R. L. Woolley, pp. 1829-1850, *ibid.*

## Figure Captions

- Figure 1. Ideal Pressure-Temperature-Composition diagram. For practical applications the length of the pressure plateau (AB) is the measure of the effective hydrogen storage capacity.
- Figure 2. Pressure-Composition Isotherms for the  $Mg_2Ni$ -H System.<sup>11</sup>
- Figure 3. Pressure Composition Isotherms for a mixed phase  $Mg_2Ni$ -Mg alloy.<sup>11</sup> Arrow indicates predicted appearance of upper plateau based on alloy composition. The presence of  $Mg_2Ni$  has a catalytic effect on the Mg-H system.
- Figure 4. Pressure Composition Isotherms for the FeTi-H System;<sup>16</sup>  
← Desorption, → Sorption.
- Figure 5. Pressure Composition Isotherms for FeTi alloys with varying Mn contents.<sup>20</sup>
- Figure 6. Pressure Composition Isotherms for the  $TiCr_{1.8}$  (Cl5)-H System.<sup>29</sup>
- Figure 7. Pressure Composition Isotherms for four  $TiCr_{2-x}Mn_x$  alloy hydrogen systems.<sup>30</sup> Value of x noted below corresponding isotherm.
- Figure 8. Pressure Composition Isotherms for the  $LaNi_5$ -Hydrogen System.<sup>3</sup>
- Figure 9. Variation of  $\Delta G$  (plateau region) with the radius of the interstitial hole as determined by Lundin et al.<sup>8</sup>
- Figure 10. Schematic showing integration of a metal hydride (e.g.,  $FeTiH_2$ ) with an energy conversion device (internal combustion engine, fuel cell, gas turbine, etc.).
- Figure 11. Proposed Multifuel Vehicle.<sup>36</sup> Design specified total vehicle weight of 1815 kg with 171 kg of FeTi. Estimated range using  $H_2$  only was 56 km. Total range,  $H_2$  + gasoline, ~325 km. Buchner and Saufferer<sup>34</sup> have recently built and tested a similar vehicle.

Figure 12. Flow diagram of peak shaving demonstration plant built by Public Service Electric and Gas Corp. (PSE&G).<sup>36</sup>

Figure 13. Iron Titanium Hydride Reservoir used in PSE&G pilot plant<sup>36</sup> (see Table 5).

Figure 14. Simple heat pump flow diagram. Heat is used at ambient temperature to decompose hydride in evaporator bed. The evolved hydrogen is compressed and reacted with dehydrided metal at a higher temperature and pressure. The flows are reversed when the evaporator bed is exhausted and the condenser bed is saturated. If 2 different hydrides having matched properties are used the mechanical compressor can be eliminated as demonstrated by Gruen et al.<sup>45</sup>

|   |            |    |          |    |          |
|---|------------|----|----------|----|----------|
| 1 | 2-526-79   | 6  | 2-523-79 | 11 | 1-795-74 |
| 2 | 2-689-68   | 7  | 2-524-79 | 12 | 1-797-74 |
| 3 | 3-198-68   | 8  | 7-722-76 | 13 | 1-675-74 |
| 4 | 1-616-73   | 9  | 2-525-79 | 14 | 6-618-76 |
| 5 | 11-1284-77 | 10 | 6-52-73  |    |          |

Table 1

Properties of MgH<sub>2</sub> and Mg<sub>2</sub>NiH<sub>4</sub>

Thermodynamic data @ 298K

| Compound                         | $\Delta H_f^\circ$<br>kcal/mol H <sub>2</sub> | $\Delta G_f^\circ$<br>kcal/mol H <sub>2</sub> | $\Delta S_f^\circ$<br>e.u./mol H <sub>2</sub> | A <sup>a</sup> | B <sup>a</sup> | Ref. |
|----------------------------------|---|---|---|----------------|----------------|------|
| MgH <sub>2</sub>                 | -18.5   | -8.7  | -33   | -4043          | 7.224          | 11   |
| Mg <sub>2</sub> NiH <sub>4</sub> | -15.4 <sup>b</sup>                            | -6.7 <sup>b</sup>                             | -29.2 <sup>b</sup>                            | -7736          | 14.7106        | 11   |

Crystal Structure, 298K

Density

N<sub>H</sub><sup>c</sup>

g/ml

MgH<sub>2</sub> = Tetragonal, a = 4.5168, c = 3.0205 Å

1.45

6.6

10

Mg<sub>2</sub>NiH<sub>4</sub> = Tetragonal, a = 6.464, c = 7.033 Å

2.57

5.7

11

<sup>a</sup> Constants in equation  $\ln P_{\text{atm}} = (A/T) + B$ <sup>b</sup> The standard state of the starting solid is taken as Mg<sub>2</sub>Ni<sup>c</sup> N<sub>H</sub> × 10<sup>22</sup> = number of H atoms/ml

Table 3

Formation of Iron Titanium Alloy Hydrides

| Thermodynamic data                                       |                                 |                              |                                 |       |         |       |
|--|---------------------------------|------------------------------|---------------------------------|-------|---------|-------|
| Relative Partial Molal Quantities Per g Atom of H @ 298K |                                 |                              |                                 |       |         |       |
| Composition  | $(\bar{H}_H - 1/2H_{H2}^\circ)$ | $(\bar{S}_H - 1/2S_H^\circ)$ | $(\bar{G}_H - 1/2G_{H2}^\circ)$ | A*    | B*      |       |
|  | kcal                            | e.u.                         | kcal                            |       |         |       |
| FeTiH <sub>0.1</sub> -FeTiH <sub>1.04</sub>              | -3.36                           | -12.7                        | 0.42                            | -5383 | 12.7612 | 16    |
| FeTiH <sub>1.20</sub>                                    | -3.70                           | -14.4                        | 0.57                            | -3728 | 14.4327 | 16    |
| FeTiH <sub>1.40</sub>                                    | -3.98                           | -15.6                        | 0.65                            | -4020 | 15.6610 | 16    |
| FeTiH <sub>1.60</sub>                                    | -4.03                           | -15.8                        | 0.68                            | -4057 | 15.9165 | 16    |
| Density  |                                 |                              |                                 |       |         |       |
| FeTiH <sub>1.0</sub> = 5.88 g/ml                         |                                 |                              |                                 |       |         | 16    |
| FeTiH <sub>1.93</sub> = 5.47 g/ml                        |                                 |                              |                                 |       |         | 16    |
| Crystal Structure FeTiD <sub>x</sub> , 298K              |                                 |                              |                                 |       |         |       |
| FeTiD <sub>1.0</sub> = orthorhombic                      |                                 |                              |                                 |       |         |       |
|  | a = 2.956Å                      | b = 4.543Å                   | c = 4.388Å                      |       |         | 25,27 |
| FeTiD <sub>1.9</sub> = monoclinic                        |                                 |                              |                                 |       |         |       |
|  | a = c = 4.7044Å                 | b = 2.8301Å                  | β = 96.57°                      |       |         | 26    |

Table 5

LOW TEMPERATURE ACTIVATION EXPERIMENTSTiFe<sub>x</sub>Mn<sub>y</sub> ALLOYSH<sub>2</sub> Pressure = 34 atm.

| <u>Alloy<br/>Composition</u>            | <u>Maximum Outgassing<br/>Temperature<br/>(°C)</u> | <u>Elapsed Time<br/>(hr)</u> | <u>Final<br/>H/Ti</u> | <u>%<br/>Reaction</u> |
|---|--|------------------------------|-----------------------|-----------------------|
| TiFe                                    | 200  | 72                           | 0.0                   | 0                     |
| TiFe <sub>0.9</sub> Mn <sub>0.096</sub> | 25   | 19                           | 1.72                  | 96                    |
| TiFe <sub>0.85</sub> Mn <sub>0.15</sub> | 25   | 6                            | 1.94                  | 100                   |
| TiFe <sub>0.8</sub> Mn <sub>0.2</sub>   | 25   | 45                           | 1.16                  | 60                    |
| TiFe <sub>0.7</sub> Mn <sub>0.2</sub>   | 50   | 3.5                          | 1.79                  | 94                    |
| TiFe <sub>0.77</sub> Mn <sub>0.09</sub> | 25   | 27.5                         | 1.79                  | 100                   |
| TiFe <sub>0.73</sub> Mn <sub>0.13</sub> | 25   | 19                           | 1.82                  | 100                   |

Table 6

Relative Partial Molal Quantities Per Gram-Atom of  
Hydrogen at 298K for the Formation of  $\text{TiCr}_{1.8}\text{H}_x$

| Compn.                             | $(\bar{H}_H - 1/2H_{H_2}^{\circ})$<br>kcal | $(\bar{S}_H - 1/2S_{H_2}^{\circ})$<br>eu | $(\bar{G}_H - 1/2G_{H_2}^{\circ})$<br>kcal | A <sup>a</sup> | B <sup>a</sup> |
|------------------------------------|--|--|--|----------------|----------------|
| $\text{TiCr}_{1.8}\text{H}_{0.84}$ | -2.06                                      | - 9.6                                    | +0.79                                      | -2077          | +9.6263        |
| $\text{TiCr}_{1.8}\text{H}_{1.68}$ | -2.41                                      | -13.2                                    | +1.53                                      | -2428          | +13.3192       |
| $\text{TiCr}_{1.8}\text{H}_{2.66}$ | -2.32                                      | -14.2                                    | +1.91                                      | -2332          | +14.2772       |
| $\text{TiCr}_{1.8}\text{H}_{2.94}$ | -2.18                                      | -15.0                                    | +2.30                                      | -2195          | +15.1265       |
| $\text{TiCr}_{1.8}\text{H}_{3.22}$ | -2.04                                      | -14.4                                    | +2.24                                      | -2058          | +14.4869       |

<sup>a</sup>Constants in  $\ln P_{\text{atm}} = (A/T) + B$

Crystal Structure 298K

Orthorhombic  $a = 7.30$ ,  $b = 5.18$   $c = 4.94 \text{ \AA}$



Table 7

Properties of Lanthanum Nickel Hydride and Mischmetal Nickel Hydride

| Compound                                      | Thermodynamic data a 298K |                         |                         | b     |        | Ref. |
|---|---------------------------|-------------------------|-------------------------|-------|--------|------|
|   | $\Delta H_f^\circ$        | $\Delta G_f^\circ$      | $\Delta S_f^\circ$      | A     | B      |      |
|   | kcal/mol H <sub>2</sub>   | kcal/mol H <sub>2</sub> | e.u./mol/h <sub>2</sub> |       |        |      |
| LaNi <sub>5</sub> H <sub>6</sub> <sup>c</sup> | -7.2                      | 0.15                    | -26                     | -3623 | 13.074 | 31   |
| R.E.Ni <sub>5</sub>                           | -5.0                      | 1.9                     | -23                     | -2516 | 11.575 | 13   |

Crystal Structure, 298K

Density

N<sub>H</sub>

g/ml

|                                  |                                  |     |     |    |
|----------------------------------|----------------------------------|-----|-----|----|
| LaNi <sub>5</sub> H <sub>6</sub> | hexagonal a = 5.440Å, c = 4.310Å | 6.5 | 5.4 | 29 |
|----------------------------------|----------------------------------|-----|-----|----|

<sup>a</sup>From the hydrogen saturated alloy<sup>b</sup>Constants in equation  $\ln P_{\text{atm}} = (A/T) + B$ <sup>c</sup>R.E. represents rare earth mixture (Mischmetal)

Table 8

Comparison of Hydrogen Storage Media

| Medium   | Effective Hydrogen Content<br>Wt % | Volumetric Hydrogen Content<br>g/ml of vol | Energy Density <sup>b</sup><br>Heat of Combustion<br>(higher) |               | Raw Materials Alloy Cost<br>\$/kg        |
|--|------------------------------------|--|---|---------------|--|
|  |                                    |  | cal/g   | cal/ml of vol |  |
| MgH <sub>2</sub> <sup>a</sup>                        | 7.0                                | 0.101                                      | 2373  | 3423          | ~2.86                                    |
| Mg <sub>2</sub> NiH <sub>4</sub>                     | 3.16                               | 0.081                                      | 1071  | 2745          |  |
| VH <sub>2</sub>                                      | 2.07                               |  | 701   |               |  |
| FeTiH <sub>1.95</sub>                                | 1.75                               | 0.096                                      | 593   | 3245          | 3.08 <sup>32</sup>                       |
| TiFe <sub>.7</sub> Mn <sub>.2</sub> H <sub>1.9</sub> | 1.72                               | ~0.09                                      | 583   | ~3050         |  |
| LaNi <sub>5</sub> H <sub>7.0</sub>                   | 1.37                               | 0.089                                      | 464   | 3051          | 17.26 Pres. <sup>32</sup><br>9.45 Future |
| R.E.Ni <sub>5</sub> H <sub>6.5</sub> <sup>c</sup>    | 1.35                               | ~0.09                                      | 458   | ~3050         | 5.95 <sup>32</sup>                       |
| Liquid H <sub>2</sub>                                | 100                                | 0.07                                       | 33900   | 2373          |  |
| Gaseous H <sub>2</sub>                               | 100                                | 0.007                                      | 33900   | 244           |  |
| N-Octane   |                                    |  | 11400   | 8020          |  |

<sup>a</sup>Starting alloy 94% Mg 6% Ni

<sup>b</sup>Refers to H only in metal hydrides

<sup>c</sup>R.E. = Mischmetal

Table 9

Energy Density ComparisonAutomotive Power SourcesActual and Proposed

| Power Source                                    | Energy Density<br>whr/kg | Conversion Efficiency<br>% | Net<br>whr/kg | Ref. |
|---|--------------------------|----------------------------|---------------|------|
| Pb/acid Battery                                 |                          |                            |               |      |
| Present   | 30                       | 70                         | 21.0          | 63   |
| Advanced  | 50                       | 70                         | 35.0          | 63   |
| Li/MS Battery                                   | 150                      | 70                         | 105           | 63   |
| FeTiH <sub>1.7</sub> <sup>a,b</sup>             | 516                      | 30                         | 154           |      |
| Mg <sub>2</sub> NiH <sub>4</sub> <sup>a,b</sup> | 1121                     | 30                         | 336           |      |
| MgH <sub>2</sub> (10% Ni) <sup>a,b,c</sup>      | 2555                     | 30                         | 767           |      |
| Gasoline <sup>a</sup>                           | 12880                    | 23                         | 2962          |      |

<sup>a</sup>No allowance for container weight

<sup>b</sup>Based on available hydrogen

i.e., FeTiH<sub>1.7</sub> → FeTiH<sub>0.1</sub>

Mg<sub>2</sub>NiH<sub>4</sub> → Mg<sub>2</sub>NiH<sub>0.3</sub>

MgH<sub>2</sub> → MgH<sub>0.05</sub>

<sup>c</sup>Nickel present as Mg<sub>2</sub>NiH<sub>4</sub>

Table 10

Hydrogen Powered Vehicles

| Vehicle Type   | Manufacturer           | Total Vehicle Wt. kg | Hydride Wt. kg  | Range km             | Ref. |
|----------------|------------------------|----------------------|---|----------------------|------|
| Jeep           | AMC <sup>a</sup>       | 1584                 | 176(FeTi)   | 113 <sup>b</sup>     | 64   |
| Bus            | Winnebago <sup>a</sup> | 4090                 | 1002(FeTi)  | 121                  | 62   |
| Bus            | Argosy <sup>a</sup>    | -                    | 907(Ti <sub>55</sub> Fe <sub>44</sub> Mn <sub>5</sub> ) | 129-274 <sup>c</sup> | 65   |
| Experimental   | Daimler-Benz           | -                    | 200(FeTi)   | 100-150              | 34   |
| Bus (Dual Bed) | Daimler-Benz           | -                    | 66(Mg2Ni)<br>133(FeTi)                                  |                      | 34   |
| Sedan (Hybrid) | Daimler-Benz           | -                    | 100(FeTi)<br>50(Gasoline)                               | -                    | 34   |

a-Converted to hydrogen fuel by Billings Energy Corp., Provo, Utah.

b-Level road, constant speed of 88 km/hr.

c-Estimated for Level road, constant speed of 88 km/hr.

Table 11

Comparison of Iron Titanium Alloy Storage Systems<sup>19</sup>

For Utility Load Levelling

|                       | <u>Full Scale Plant</u>              |                           |                                       |
|-----------------------|--------------------------------------|---------------------------|---------------------------------------|
|                       | <u>PSE &amp; G<br/>Demonstration</u> | <u>Current<br/>Design</u> | <u>Advanced<br/>Design</u>            |
| Alloy                 | FeTi                                 | FeTi                      | TiFe <sub>0.7</sub> Mn <sub>0.2</sub> |
| Wt % Hydrogen Stored  | 1.57                                 | 1.15                      | 1.60                                  |
| Charging Press. atm.  | 35                                   | 30                        | 10                                    |
| Discharge Press. atm. | 2                                    | 2                         | 2                                     |
| Hot Water Temp. °C    | 45 .                                 | 160                       | 160                                   |
| Cold Water Temp °C    | 17                                   | 30                        | 30                                    |

Table 12

Tritium-Hydrogen Separation Factor<sup>50,51</sup>

| Hydride   | Temp, °C | Separation+<br>Factor<br>$\alpha$ |
|---|----------|-----------------------------------|
| TiH <sub>2</sub>  | 350      | 0.67                              |
| TiVH <sub>4.15</sub>                                    | 40       | 1.18                              |
| TiCrH <sub>2.35</sub>                                   | 40       | 1.54                              |
| TiCr <sub>2</sub> H <sub>1.68</sub>                     | -20      | 2.01                              |
| TiCr <sub>2</sub> H <sub>1.48</sub>                     | 0        | 2.03                              |
| TiCrMnH <sub>2.19</sub>                                 | -20      | 2.05                              |
| TiCrMnH <sub>1.28</sub>                                 | 0        | 1.80                              |
| Ti <sub>2</sub> MoH <sub>4.77</sub>                     | 40       | 1.61                              |
| TiMoH <sub>2.99</sub>                                   | 40       | 1.61                              |
| TiMo <sub>2</sub> H <sub>1.10</sub>                     | -20      | 1.87                              |
| TiMnH <sub>1.99</sub>                                   | 40       | 1.37                              |
| FeTiH <sub>1.88</sub>                                   | 0        | 0.92                              |
| FeTiH <sub>1.69</sub>                                   | 0        | 0.95                              |
| FeTiH <sub>1.21</sub>                                   | 40       | 1.0                               |
| Fe <sub>0.6</sub> TiMn <sub>0.2</sub> H <sub>1.67</sub> | 40       | 1.0                               |
| TiCoH <sub>1.44</sub>                                   | 40       | 0.85                              |
| TiNiH <sub>1.44</sub>                                   | 40       | 0.74                              |
| VH <sub>0.65</sub>                                      | 210      | 1.10                              |
| VH <sub>0.85</sub>                                      | 30.6     | 1.40                              |
| VH <sub>2</sub>   | 0        | 1.91                              |
| VH <sub>2</sub>   | 0        | 1.96                              |
| VH <sub>2</sub>   | 28.0     | 1.72                              |

Table 12 (cont'd)

Tritium-Hydrogen Separation

| Hydride   | Temp, °C | Separation+<br>Factor<br>$\alpha$ |
|---|----------|-----------------------------------|
| VH <sub>2</sub>                                   | 28.2     | 1.70                              |
| VH <sub>2</sub>                                   | 28.2     | 1.77                              |
| VH <sub>2</sub>                                   | 28.2     | 1.77                              |
| VH <sub>2</sub>                                   | 45.2     | 1.61                              |
| Mg <sub>2</sub> NiH <sub>4</sub>                  | 325      | 0.46                              |
| Mg <sub>2</sub> NiH <sub>4</sub>                  | 251      | 0.48                              |
| LaNi <sub>5</sub> H <sub>6.6</sub>                | 0        | 1.25                              |
| LaNi <sub>5</sub> H <sub>6.6</sub>                | 29-30    | 1.23                              |
| LaNi <sub>5</sub> H <sub>6.6</sub>                | 27.7     | 1.12                              |
| LaNi <sub>5</sub> H <sub>6.6</sub>                | 47.0     | 1.09                              |
| R.E.Ni <sub>5</sub> H <sub>6-6</sub> *            | 0        | 1.29                              |
| R.E.Ni <sub>5</sub> H <sub>6-6</sub> *            | 0        | 1.29                              |
| V <sub>0.9</sub> Cr <sub>0.1</sub> H <sub>2</sub> | 28.4     | 1.66                              |
| ZrNiH <sub>3</sub>                                | 27.6     | 1.05                              |

\*R.E. = mischmetal: Ce, 50%; La, 27%; Nd, 16%; Pr, 5%, other rare earths, 2%.

+  $\alpha$  = (T/H)<sub>solid</sub>/(T/H)<sub>gas</sub>

Table 13

Ignition Temperature of Various Materials in Air

| Material                         | Particle Size $\mu$ | Bulk Powder | Dust Cloud | Ref. |
|----------------------------------|---------------------|-------------|------------|------|
| FeTi                             | 74-149              | No ignition |            | 60   |
| FeTi                             | <74                 |             | 490        | 60   |
| FeTiH <sub>x</sub>               | 74-149              | 188         |            | 60   |
| FeTiH <sub>x</sub>               | <74                 |             | 420        | 60   |
| LaNi <sub>5</sub>                | <74                 |             | 420        | 61   |
| LaNi <sub>5</sub> H <sub>x</sub> | 12(Avg.)            | 192         | 320        | 61   |
| U                                | <40                 | 100         | 25         | 59   |
| UH <sub>3</sub>                  | <12                 | 25          | 25         | 59   |
| Zr                               | <12                 | 190         | 25         | 59   |
| Zr                               | <40                 | 300         | 350        | 59   |
| ZrH <sub>2</sub>                 | <30                 | 340         | 430        | 59   |



1/2

EQUIL. H PRESS.

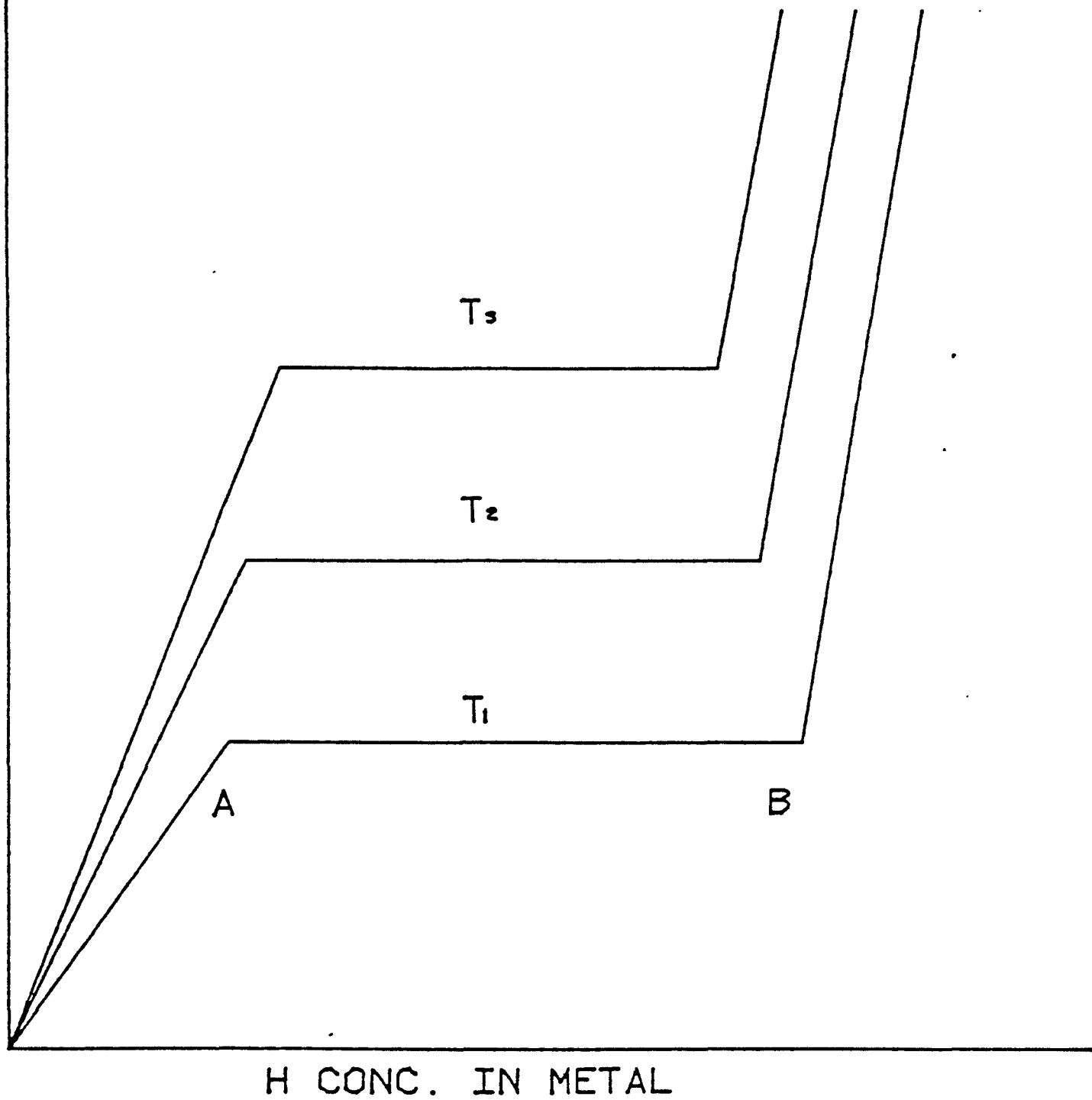


Figure 1. Ideal Pressure-Temperature-Composition diagram. For practical applications the length of the pressure plateau (AB) is the measure of the effective hydrogen storage capacity.

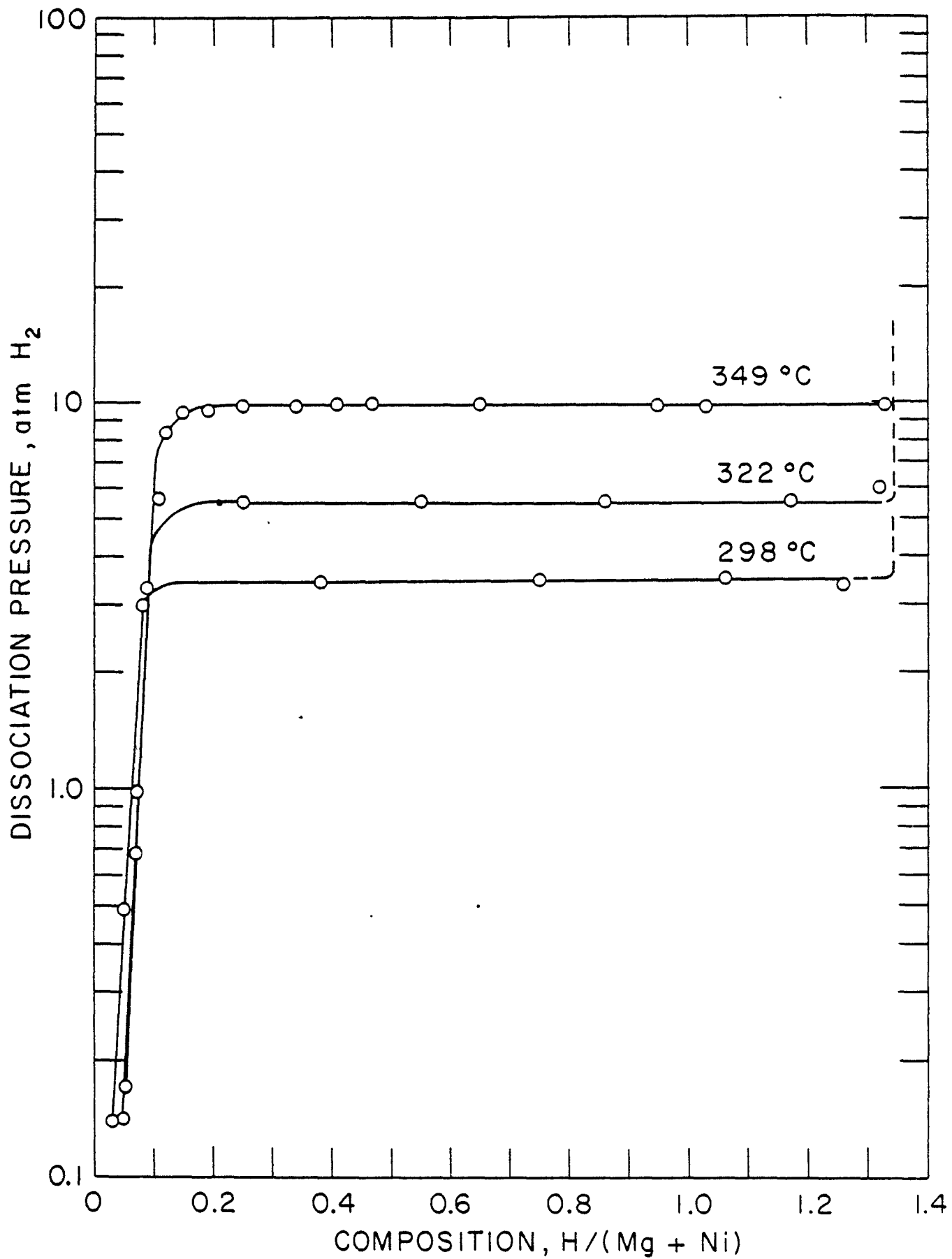


Figure 2. Pressure-Composition Isotherms for the Mg<sub>2</sub>Ni-H System.<sup>11</sup>

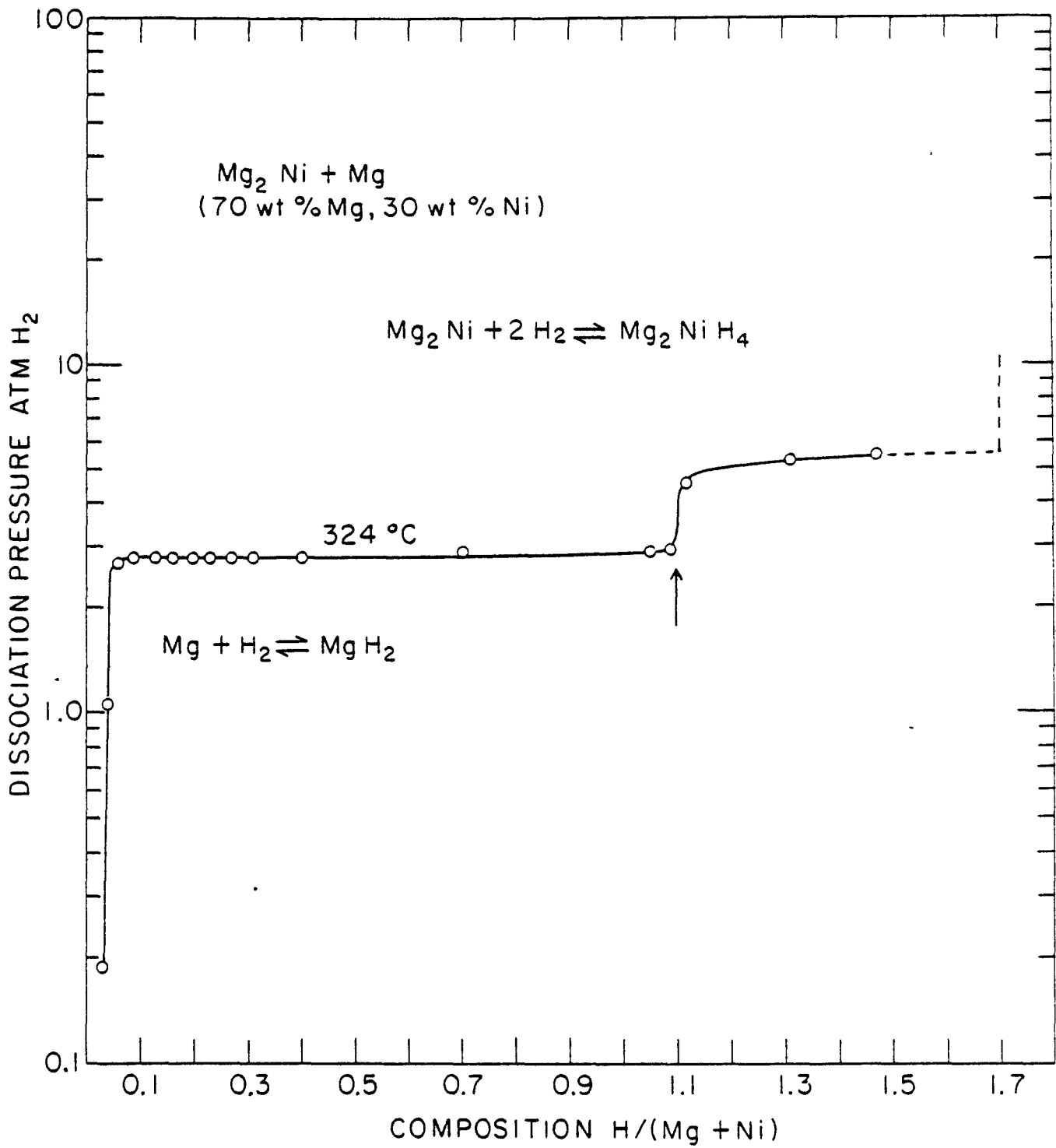


Figure 3. Pressure Composition Isotherms for a mixed phase  $\text{Mg}_2\text{Ni-Mg}$  alloy.<sup>11</sup> Arrow indicates predicted appearance of upper plateau based on alloy composition. The presence of  $\text{Mg}_2\text{Ni}$  has a catalytic effect on the Mg-H system.

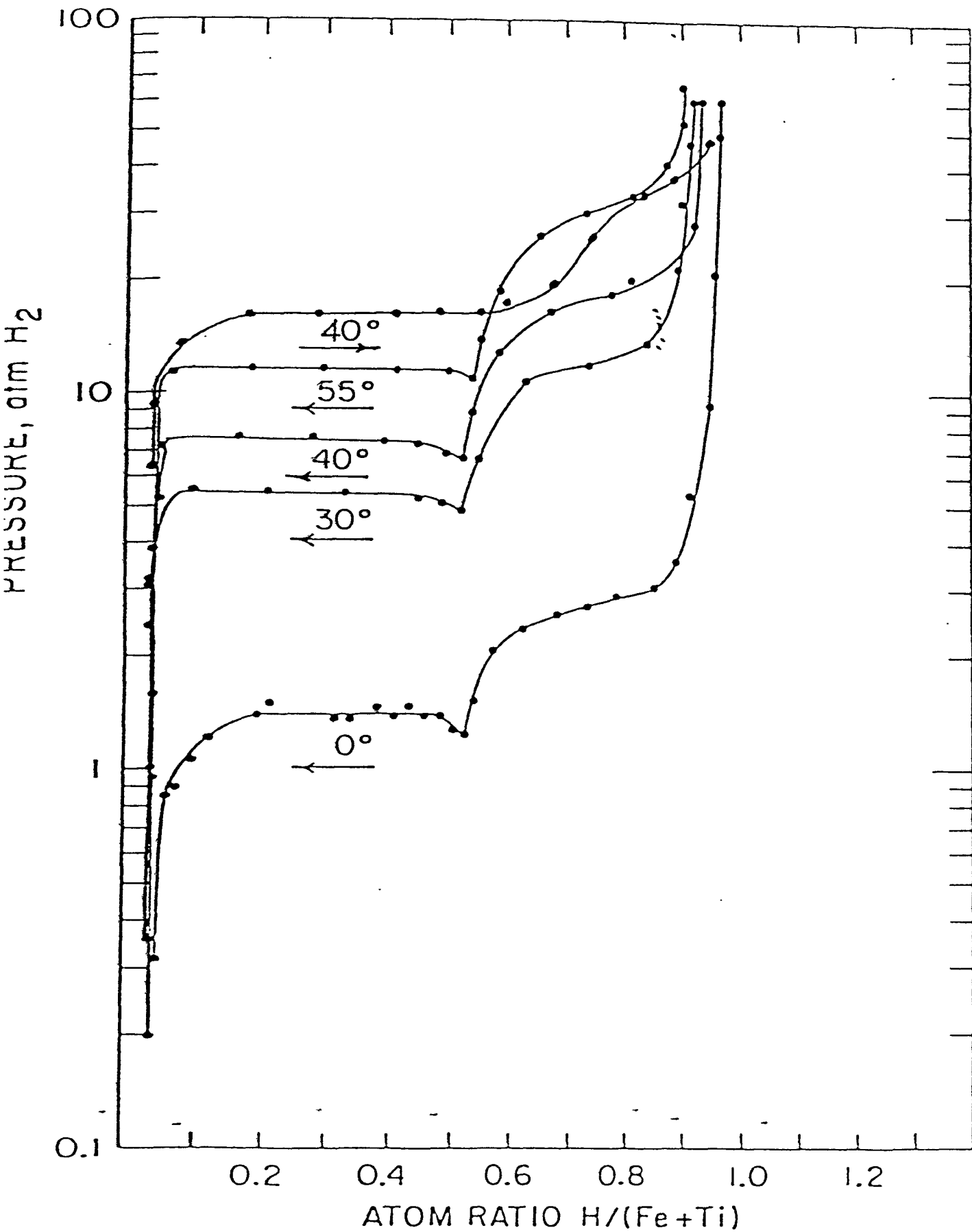


Figure 4. Pressure-Composition Isotherms for the FeTi-H System;<sup>16</sup>  
 +Desorption, +Sorption.

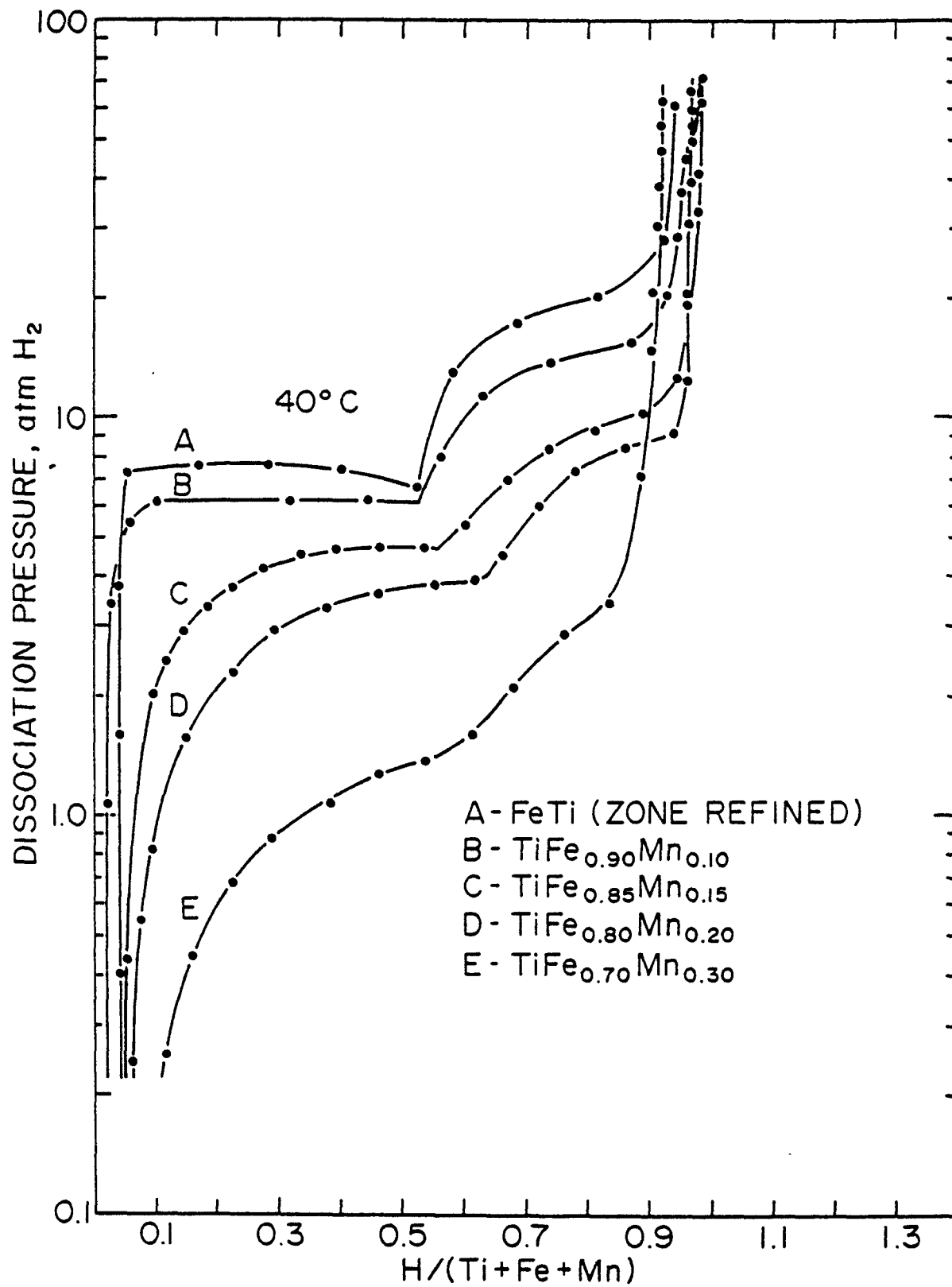


Figure 5. Pressure Composition Isotherms for FeTi alloys with varying Mn contents.<sup>20</sup>

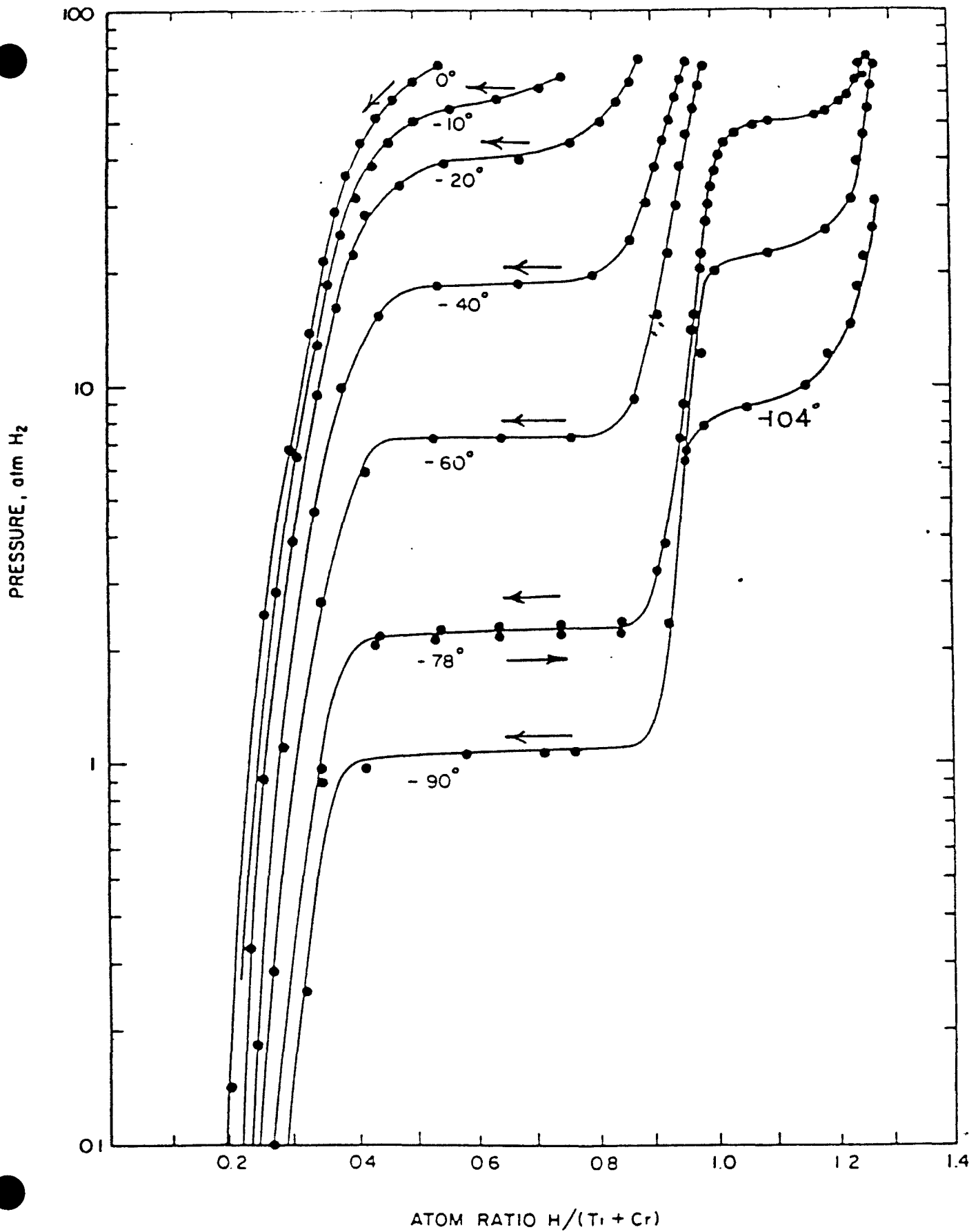


Figure 6. Pressure Composition Isotherms for the  $\text{TiCr}_{1.8}(\text{C15})\text{-H}$  System.<sup>29</sup>  
 ← Desorption, → Sorption

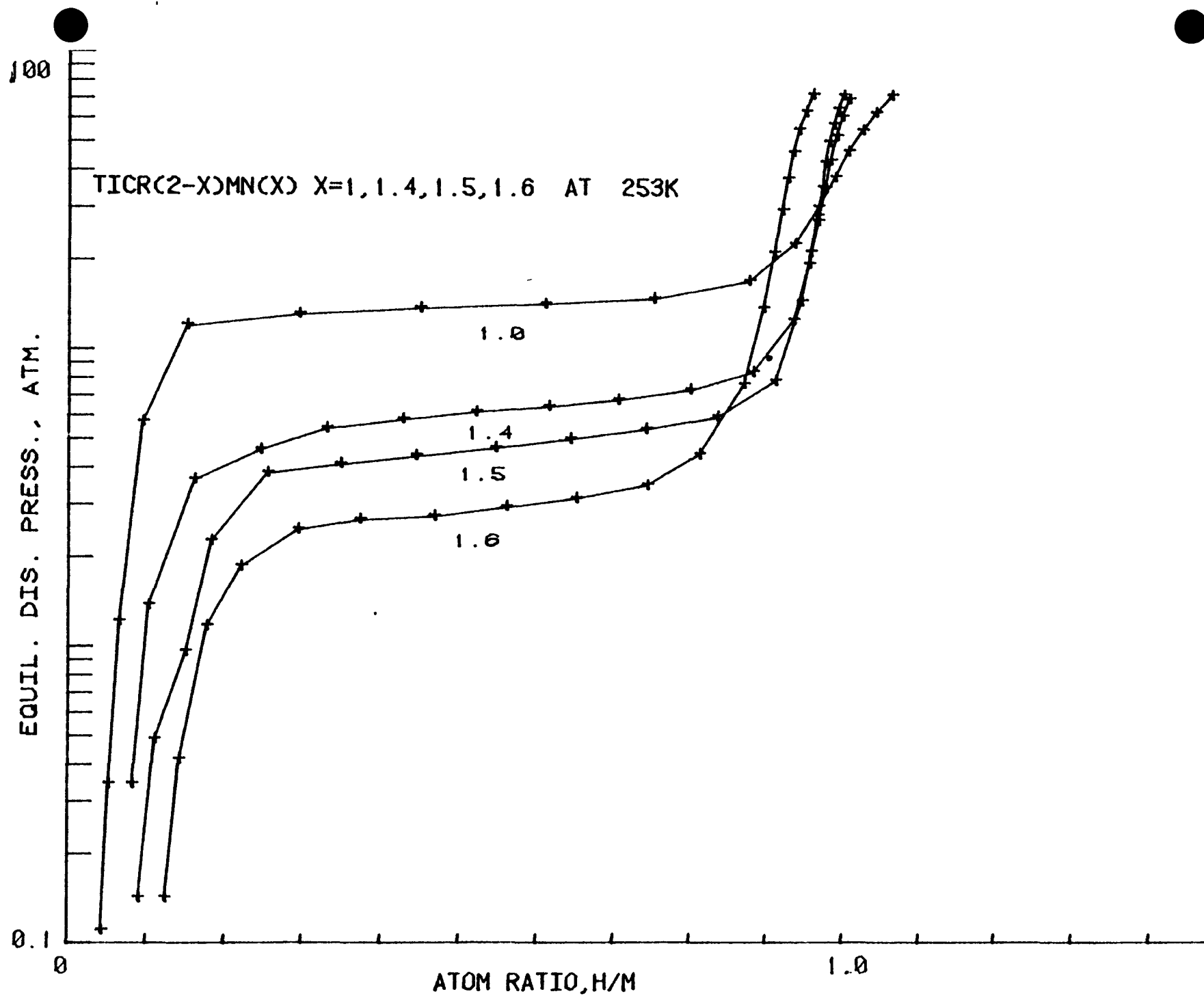


Figure 7. Pressure Composition Isotherms for four  $\text{TiCr}_{2-x}\text{Mn}_x$  alloy hydrogen systems.  
 Value of x noted below corresponding isotherm.

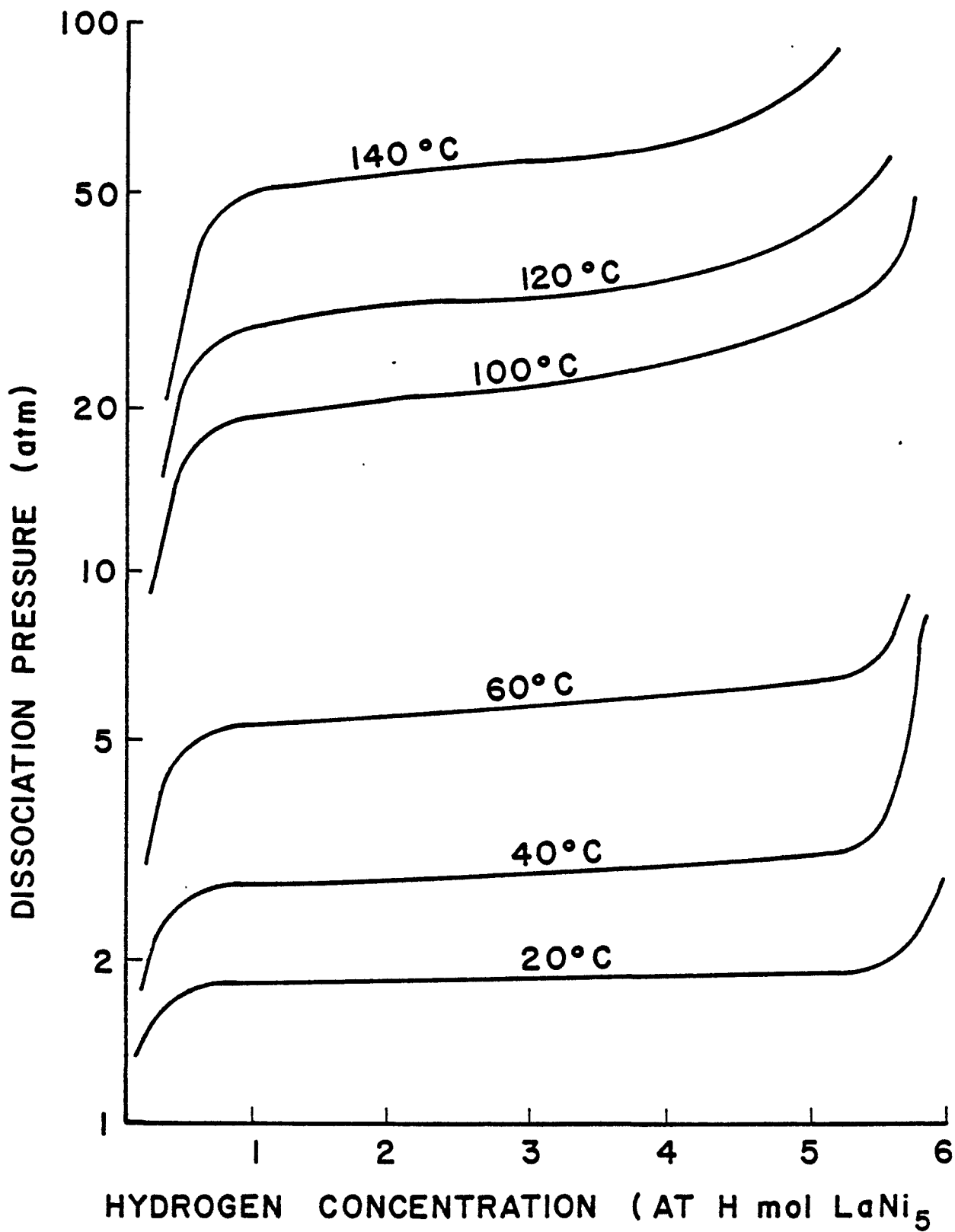


Figure 8. Pressure Composition Isotherms for the LaNi<sub>5</sub>-Hydrogen System.<sup>3</sup>



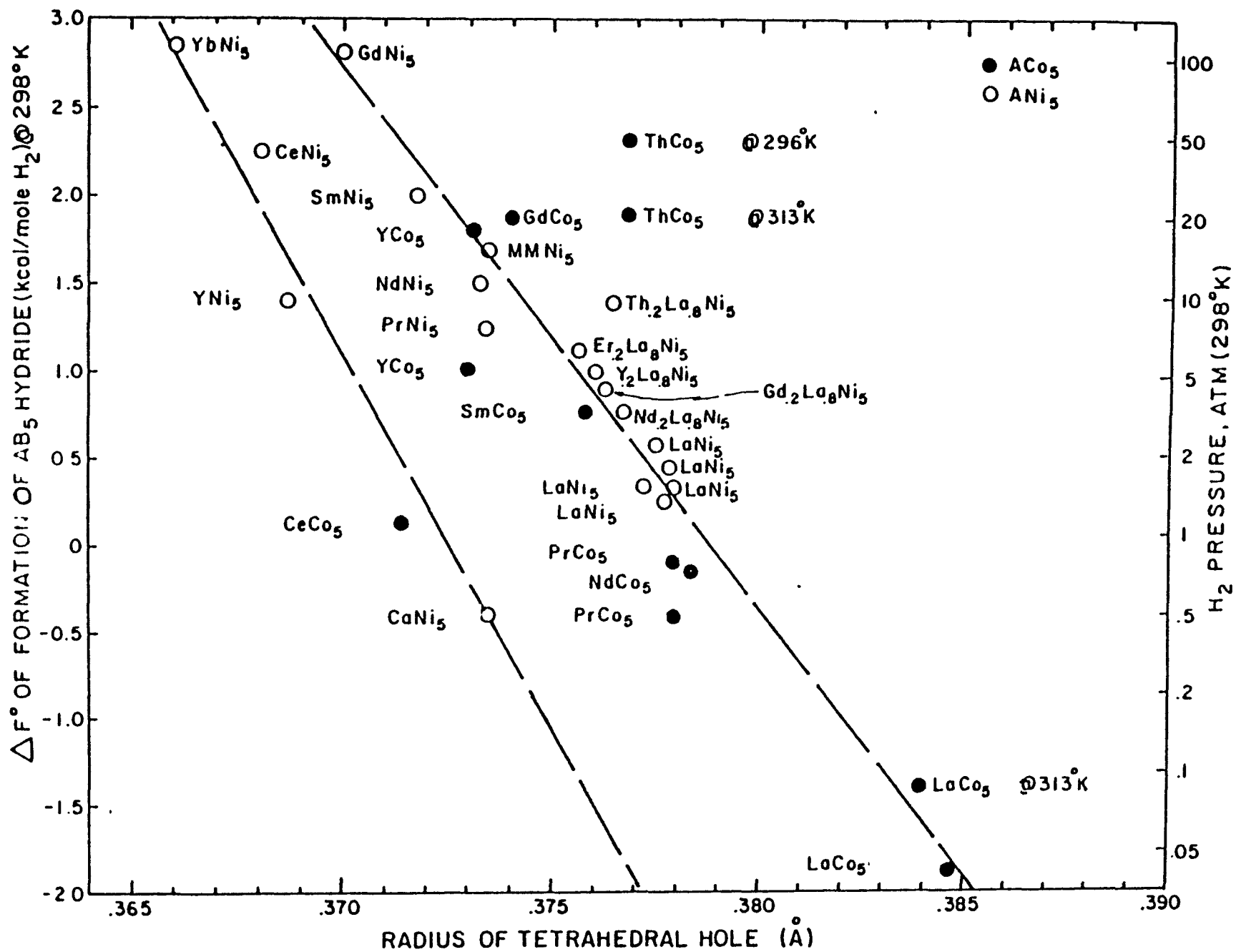


Figure 9. Variation of  $\Delta G$  (plateau region) with the radius of the interstitial hole as determined by Lundin et al.<sup>8</sup>

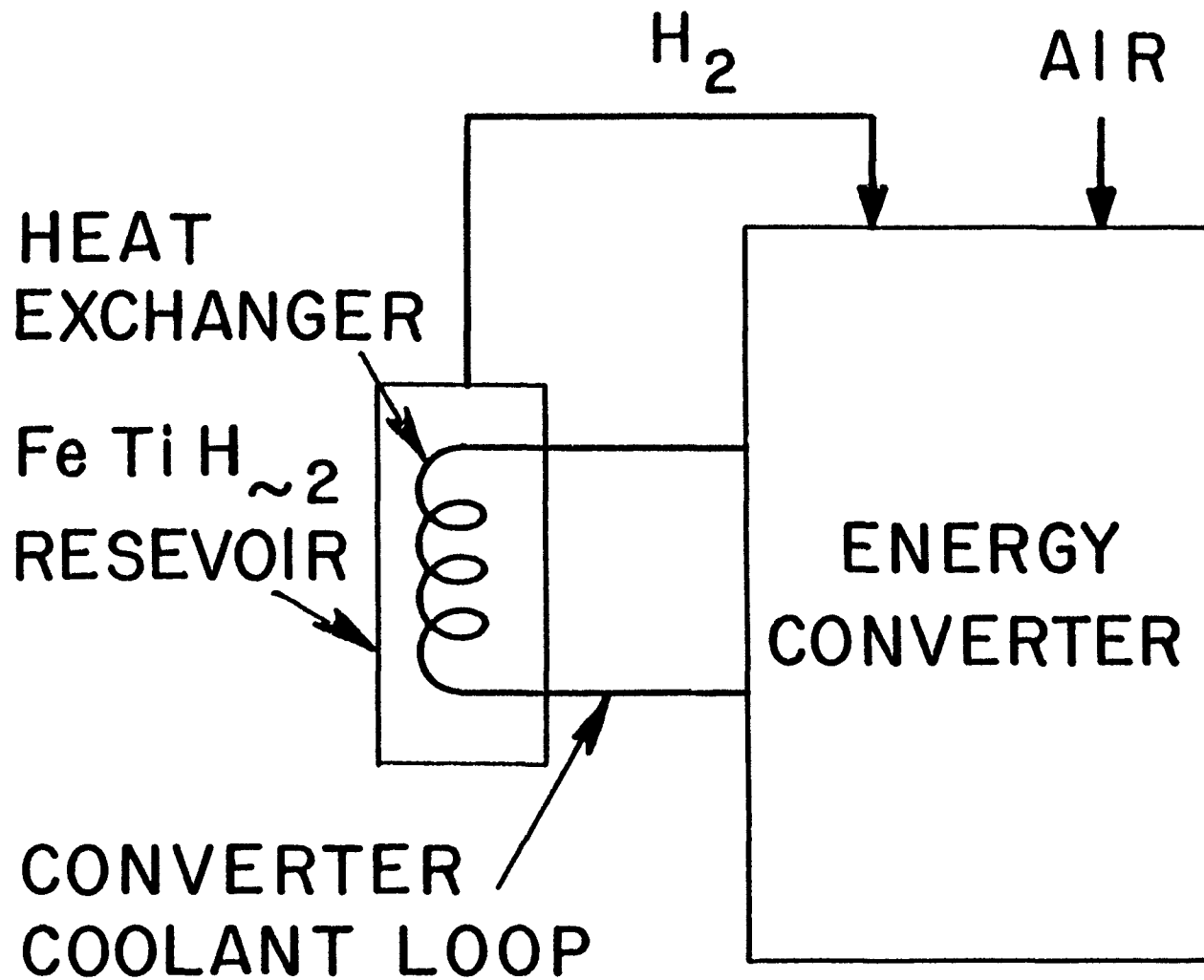


Figure 10. Schematic showing integration of a metal hydride (e.g., FeTiH<sub>2</sub>) with an energy conversion device (internal combustion engine, fuel cell, gas turbine, etc.).

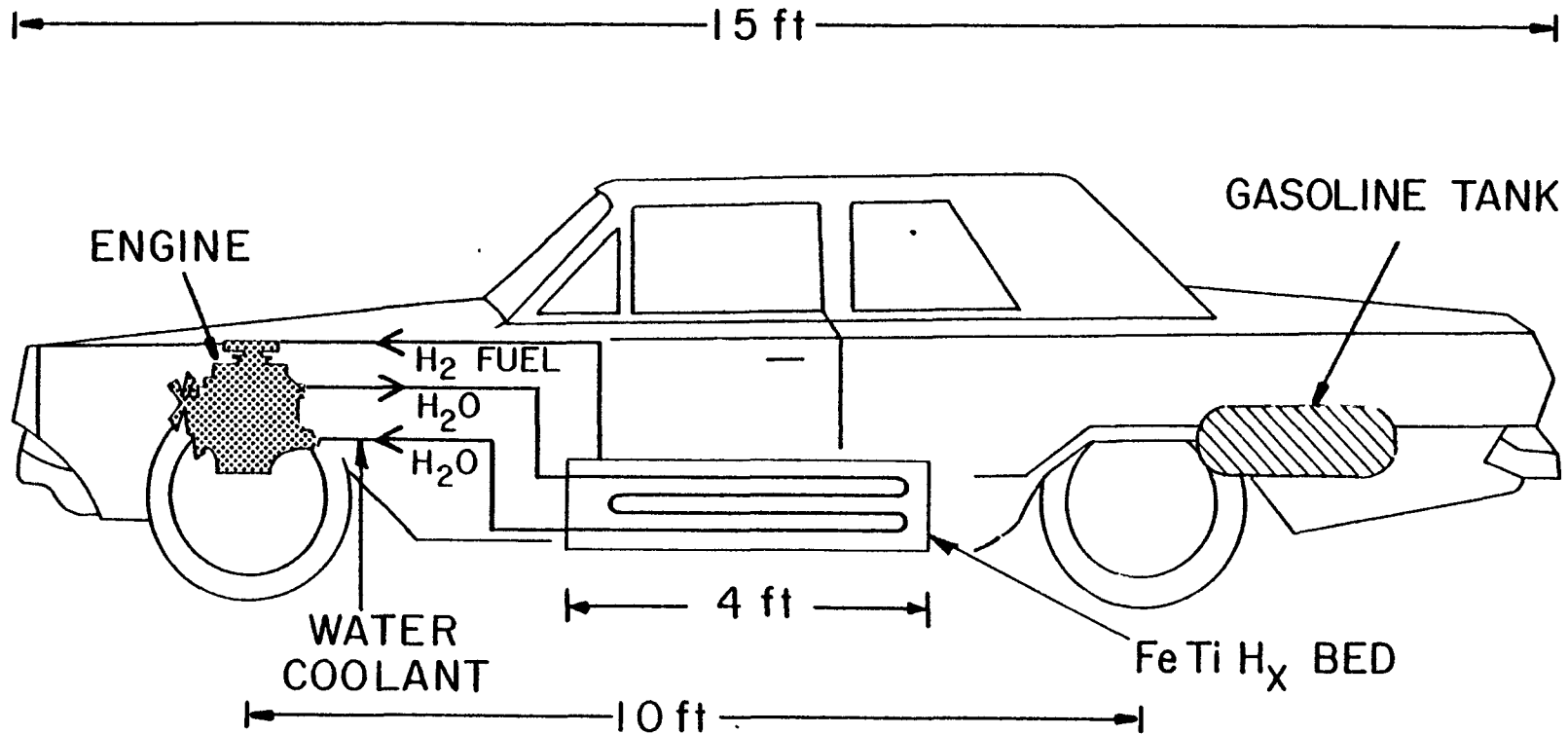
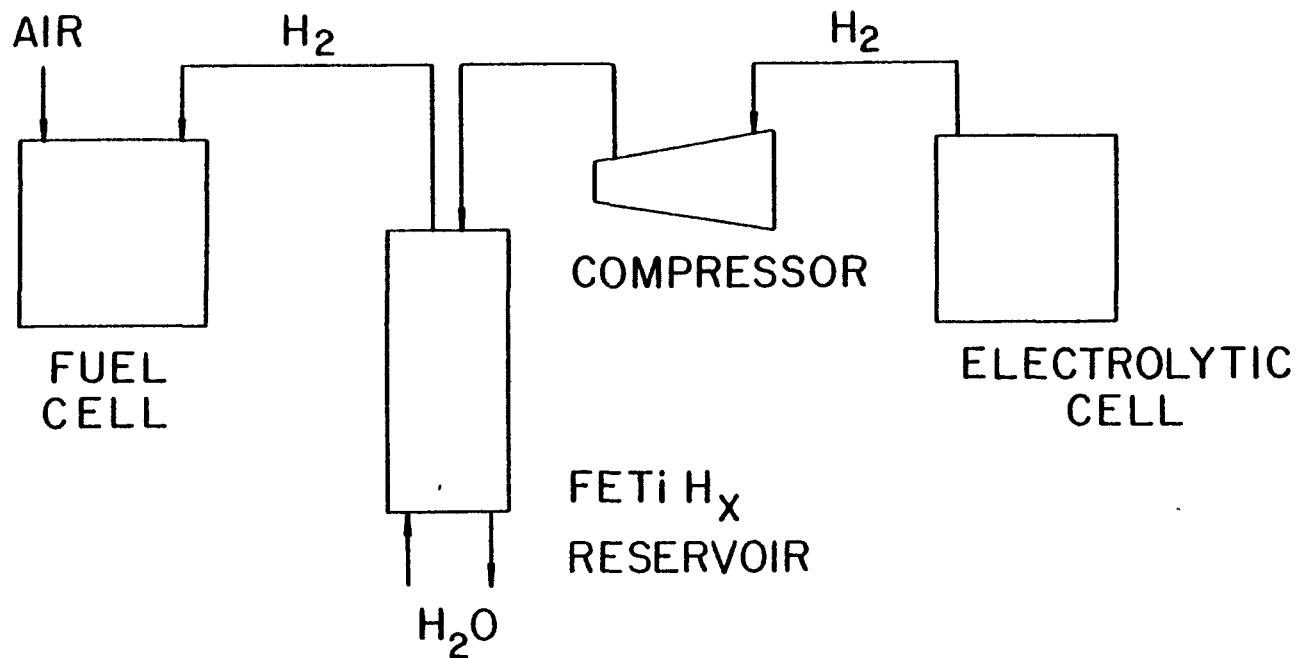


Figure 11. Proposed Multifuel Vehicle.<sup>36</sup> Design specified total vehicle weight of 1815 kg with 171 kg of FeTi. Estimated range, using H<sub>2</sub> only was 56 km. Total range, H<sub>2</sub> + gasoline, ~325 km. Buchner and Saufferer<sup>34</sup> have recently built and tested a similar vehicle.



## PSE + G PEAK SHAVING DEMONSTRATION

Figure 12. Flow diagram of peak shaving demonstration plant built by Public Service Electric and Gas Corp. (PSE&G).<sup>36</sup>

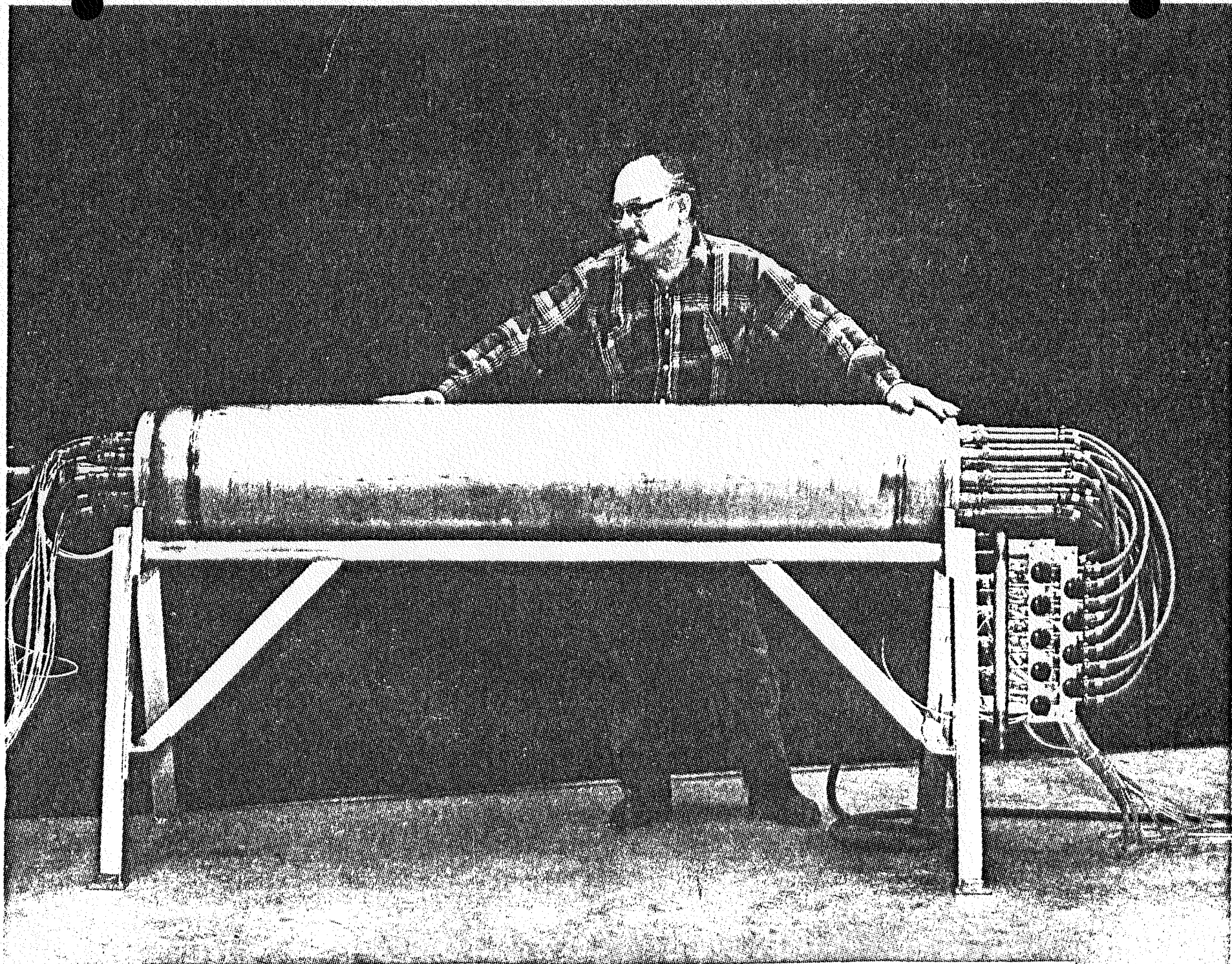


Figure 13. Iron Titanium Hydride Reservoir used in PSE&G pilot plant<sup>36</sup> (see Table 5).

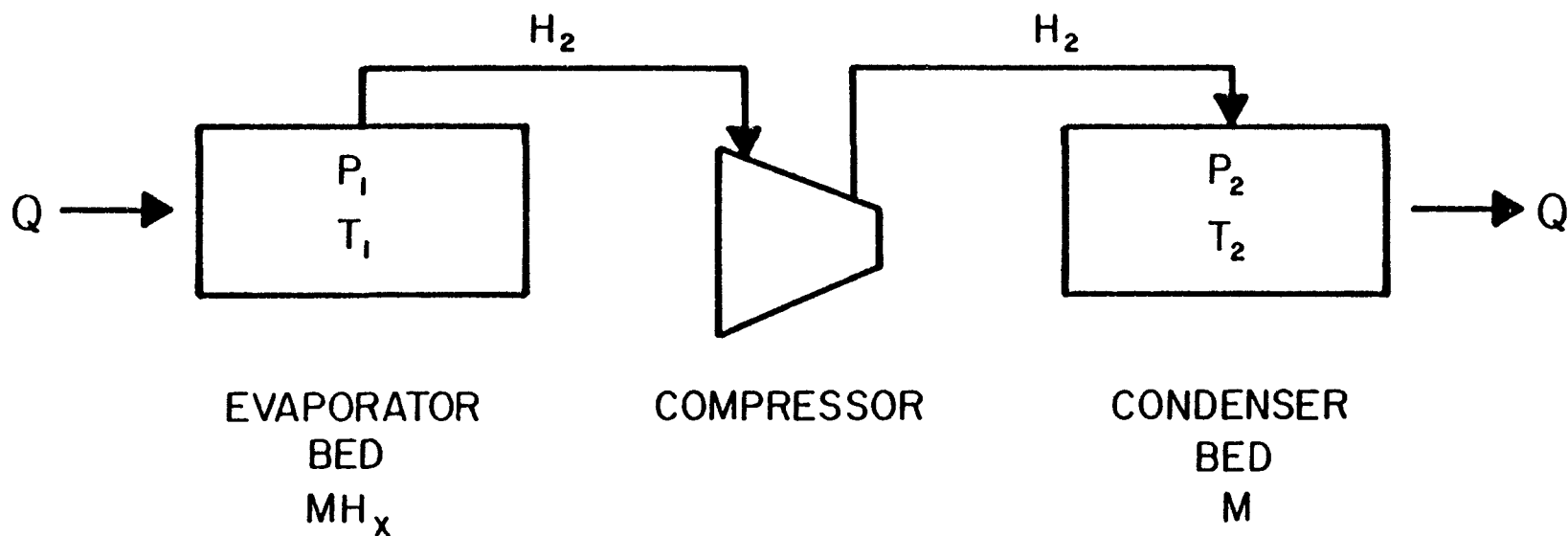


Figure 14. Simple heat pump flow diagram. Heat is used at ambient temperature to decompose hydride in evaporator bed. The evolved hydrogen is compressed and reacted with dehydrided metal at a higher temperature and pressure. The flows are reversed when the evaporator bed is exhausted and the condenser bed is saturated. If 2 different hydrides having matched properties are used the mechanical compressor can be eliminated as demonstrated by Gruen et al.<sup>45</sup>